NASA Contractor Report 180893

3-D Inelastic Analysis Methods for Hot Section Components

Fourth Annual Status Report for the Period February 14, 1986 to February 14, 1987

Volume I - Special Finite Element Models

S. Nakazawa

May 1988

Prepared for
Lewis Research Center
Under Contract NAS3-23697

National Aeronautics and
Space Administration

Report Documentation Page

1. Report No.	2. Government Accession No.	3. Recipient's Catalog No.
NASA CR-180893		

4. Title and Subtitle	5. Report Date
3-D INELASTIC ANALYSIS METHODS FOR HOT SECTION COMPONENTS - FOURTH ANNUAL REPORT Volume I, Special Finite Element Models	May 1988
	6. Performing Organization Code

7. Author(s)	8. Performing Organization Report No.
S. Nakazawa	PWA-5940-62
	10. Work Unit No.

9. Performing Organization Name and Address	11. Contract or Grant No.
UNITED TECHNOLOGIES CORPORATION Pratt & Whitney, Commercial Engineering 400 Main St., East Hartford, CT 06108	NAS3-23697
	13. Type of Report and Period Covered Fourth Annual Report 2/14/86 to 2/14/87
12. Sponsoring Agency Name and Address NATIONAL AERONAUTICS AND SPACE ADMINISTRATION Lewis Research Center 21000 Brookpark Road Cleveland, OH 44135	14. Sponsoring Agency Code RTOP 533-04-1A

15. Supplementary Notes

Project Manager, C. C. Chamis, MS 49-6
NASA-Lewis Research Center; Cleveland, OH 44135

16. Abstract

This Annual Status Report presents the results of work performed during the fourth year of the 3-D Inelastic Analysis Methods for Hot Section Components program (NASA Contract NAS3-23697). The objective of the program is to produce a series of new computer codes that permit more accurate and efficient three-dimensional analyses of selected hot section components, i.e., combustor liners, turbine blades and turbine vanes. The computer codes embody a progression of mathematical models and are streamlined to take advantage of geometrical features, loading conditions, and forms of material response that distinguish each group of selected components. Volume I of this report discusses the special finite element models that were developed during the fourth year of the contract effort.

17. Key Words (Suggested by Author(s))	18. Distribution Statement
3-D Inelastic Analysis, Finite Elements, Boundary Elements, High Temperature, Creep, Vibration, Buckling, Solution Methods, Constitutive Modeling	

19. Security Classif. (of this report)	20. Security Classif. (of this page)	21. No. of pages	22. Price
Unclassified	Unclassified	85	

PREFACE

This Annual Status Report, Volume I, describes the results of work performed on Task VB (Special Finite Element Models) during the fourth year of the NASA Hot Section Technology (HOST) program, "3-D Inelastic Analysis Methods for Hot Section Components" (Contract NAS3-23697). The finite element code, MHOST (MARC HOST), is developed further based on mixed iterative solution procedures whose concepts and basic technology were established in the first and second year efforts. The technology is extended in the current phase to incorporate the effect of multiple embedded singularities in generic modeling regions. Specifically, the local mesh refinement technology and the special function representation for singular behavior of strain are developed based on mixed element concepts. The local mesh refinement algorithm, referred to as the subelement iteration, utilizes conventional linear and higher order polynomial representations for spatial discretization.

The program is being conducted under the direction of Dr. C. C. Chamis of the NASA-Lewis Research Center. Prime contractor activities at United Technologies Corporation are managed by Dr. E. S. Todd. Subcontractor efforts on finite element tasks at MARC Analysis Research are led by Dr. J. C. Nagtegaal.

TABLE OF CONTENTS

LIST OF ILLUSTRATIONS

LIST OF TABLES

NOMENCLATURE

Alphabetical Symbol	Description
$\mathbf{a}$	Acceleration vector
a_j	Acceleration vector component
$\mathbf{B}$	Discrete gradient operator
$\bar{\mathbf{B}}$	Strain-displacement matrix
c	Geometric constant
$\mathbf{C}$	Damping matrix
$\mathbf{CS}$	Strain projection operator
d	Differential operator
$\mathbf{D}$	Material modulus matrix
D_{ijkl}	Fourth order tensor component of material modulus
$\mathbf{e}$	Nodal strain vector
E	Young's modulus
$\mathbf{f}$	Body force vector
f_j	Body force vector component
$\mathbf{F}$	Nodal force vector
$\mathbf{g}$	Gravity acceleration vector
$\mathbf{G}$	Diagonalized Gramm matrix for finite element basis
$\mathbf{G}_I$	Ith diagonal entry of diagonalized Gramm matrix
h	Thickness for plates and shells
$\mathbf{h}$	Surface loading vector
I	Functional indicator
$\mathbf{J}$	Jacobian matrix for the isoparametric transformation
$\mathbf{K}$	Displacement stiffness matrix

NOMENCLATURE (continued)

Alphabetical Symbol	Description
L	Lagrangian functional
$\mathbf{L}$	Centrifugal effects matrix
$\mathbf{M}$	Mass matrix
$\mathbf{n}$	Unit normal vector
$\mathbf{N}$	Finite element basis function
n_j	Cartesian component of the unit normal
$\mathbf{P}$	Load at a given point
q	Pressure loading
r	Radial coordinate for axisymmetric geometry
R	Radius
$\mathbf{R}$	Nodal Residual vector
$\mathbf{ROT}$	Rotation tensor
s	Line search parameter
$\mathbf{s}$	Nodal stress vector
S	Surface
t	Time
$\mathbf{t}$	Traction vector
t_j	Traction vector component
$\mathbf{u}$	Displacement vector
$\mathbf{U}$	Right stretch tensor
u_j	Displacement vector component
$\mathbf{v}$	Velocity vector
V	Space for admissible displacement variation

Alphabetical Symbol	Description
$\mathbf{v}_j$	Vector for BFGS update
v_j	Velocity vector component
w	Lateral deflection
$\mathbf{w}$	Vector for BFGS update
$\mathbf{x}$	Position vector
x_j	Cartesian component of the position vector

Greek Symbol	Description
$[\alpha]$	Yield surface center location
β	Newmark constant
δ, Δ	Incremental indicators
∇	Gradient operator
$[\epsilon]$	Strain tensor
ϵ_{ij}	Strain tensor component
ξ, η, ζ	Isoparametric coordinates
γ	Load factor for the arc-length method
λ	Eigenvalue parameter
ν	Poisson's ratio
$[\sigma]$	Stress tensor
σ_{ij}	Stress tensor component
ρ	Material density
ω	Angular (rotational) speed
Ω	Problem domain
$\partial\Omega$	Boundary of the domain

Sub- and Superscripts	Description
c (subscript)	Centrifugal effects indicator
e	Quantities defined on each element
E, EL	Elastic response
G (subscript)	Geometric effects indicator
h	Finite element approximation
i, j, k, ...	Indices for vector and tensor component (when used as subscripts); iteration and incrementation counter (when used as superscripts, also sometimes when used as subscripts with bold face indicators)
I, J, K, ...	Nodal point counter
MAX	Maximum number
PL	Plastic response
R (subscript)	Recovery process indicator
S (subscript)	Shear, transverse shear component
t (superscript)	Time indicator
T (subscript)	Tangent
T (superscript)	Transpose of matrix
-1 (superscript)	Inverse of matrix
0,o	Initial state indicator

Other

( ),	Derivative with respect to spatial (location) coordinate
( )	Derivative with respect to time

1.0 SUMMARY

The Special Finite Element Models portion of the HOST (Hot Section Technology) 3-D Inelastic Analysis Methods program is divided into two 24-month segments: a base program, and an option program exercised at the discretion of the Government. Versions 1 and 2 of MHOST (MARC-HOST) were developed during the base program (Tasks IB and IIB). The MHOST code employs both shell and solid (hexahedral) elements in a mixed iterative solution framework. This code provides comprehensive capabilities for investigating local (stress/strain) and global (vibration and buckling modes) behavior of turbine engine hot section components. In the development of MHOST, advantage has been taken of the technical expertise of engineers at MARC Analysis Research Corporation. This has led to the construction of sophisticated algorithms and codes which may reduce computer time and memory requirements for three-dimensional analyses.

Version 4 of the MHOST code has been developed under Task VB of the HOST 3-D Inelastic Analysis Methods option program. These latest development efforts have concentrated on the consolidation of the numerical technology created and implemented for the basic mixed iterative solution strategy. In addition, the subelement solution strategy designed to capture local behavior related to embedded discontinuities has been investigated further.

Efforts have been devoted to maintain the computer program on different computer systems and to improve quality. An in-core profile solution subsystem has been added, replacing the original band matrix solution. The computational procedures for eigenvalue extraction and transient time integration have been improved and been made compatible with this new solution package.

Enhancement of the solution capabilities of the MHOST code include the large displacement option to update nodal coordinates, the stress stiffening option for quasi-static and eigenvalue analysis and the centrifugal mass option for a structure rotating at a high angular velocity.

Algorithms developed for and implemented into the MHOST code utilizing the mixed global solution strategy and subelement techniques are discussed in detail in this report in conjunction with remarks on programming considerations.

2.0 LITERATURE SURVEY

This section reviews literature on the application of nonlinear finite element methods to the inelastic analysis of turbine engine hot section components. It is not intended to discuss here the state-of-the-art finite element technology but to provide a snapshot of the current trends in research and development for the period since the last annual report [NAKAZAWA (1986)]. An attempt is made in this survey to position the technology developed under the HOST contract in the computational mechanics perspective.

2.1 INTRODUCTION

The major areas of research in the improvement of computational performance and applicability of finite elements have continued to be:

1. Mixed and hybrid formulations designed to improve the accuracy of finite elements

2. Global solution procedures for linear and nonlinear finite element equations to reduce both memory requirements and the number of arithmetic operations with particular emphasis on iterative solution strategies

3. Post-processing methods designed not only to estimate errors accurately a posteriori, leading to adaptive mesh refinement strategies, but also to extract more information out of a finite element solution.

Both modern numerical technology and advanced computing machinery now allow the application of finite elements to a wider range of problem areas. The use of large meshes for representing fine detail in engineering problems has become very valuable. Sophisticated numerical methods have been developed to deal with combined nonlinear kinematics and material responses in a highly efficient manner.

This section concentrates on the reports and articles which have appeared since the previous literature survey reports [NAKAZAWA (1986) Section 3.1, and FYHRE, HUGHES (1983)].

2.2 VARIATIONAL FORMULATION AND ELEMENT TECHNOLOGY

Interest continues to remain high in using the mixed variational formulation as a basis for developing finite element methods. The Hu-Washizu principle has become the most popular variational formulation from which numerical methods are derived. It seems the most natural approach, for instance, from which to derive algorithms for probabilistic structural analysis. Evaluation methods for finite elements based upon mixed variational principles have also been developed recently. In modern literature, the words 'mixed' and 'hybrid', as

applied to finite elements, are often used interchangeably and ambiguously. Seemingly, the mixed methods derived from piecewise discontinuous stress representations are usually referred to as 'hybrid' formulations, while those derived from independent strain interpolations as well as other mixed formulations are referred to as 'mixed' forms. It is interesting to note moreover that the word 'hybrid' is even used by a certain sector of computational mechanics as referring to a class of methods combining the finite element and boundary integral formulations.

Interest in the Hu-Washizu principle has been revived in recent years by the untimely death of one of the original investigators and the subsequent publication of his memorial volume [PIAN (1984)]. Utilization of this principle for the analysis of existing methodology, such as the numerically integrated displacement formulation [ZIENKIEWICZ, NAKAZAWA (1984)], appears frequently in the literature. BELYTSCHKO (1986) presents an excellent review of the technology available for thick plate and shell element formulations based on the Reissner-Mindlin theory.

Efforts to use the mixed Hu-Washizu finite element equations as a driving mechanism for the iterative solution of linear and nonlinear problems continue as a part of the HOST project, as reported in progress reports by WILSON, BAK, NAKAZAWA, BANERJEE (1984, 1985), and NAKAZAWA (1986). Also, a number of papers discuss various aspects of this methodology [NAKAZAWA, NAGTEGAAL (1986), and NAKAZAWA, SPIEGEL (1986)].

With particular application to transient dynamics, a version of the mixed iterative solution algorithm combined with a second order, single step time integration operator has been proposed and applied to a number of linear elastic problems by ZIENKIEWICZ, LI, NAKAZAWA (1986).

An analysis of a certain class of mixed finite elements is discussed by LE TALLAC (1986). An iterative algorithm based on the Hu-Washizu principle is derived for rate-independent deviatoric plasticity. The elastic strain is used as a variable instead of the total strain. This formal alteration of the formulation, in conjunction with the radial return algorithm being hardwired to the analysis, enabled Le Tallac to discuss the solution existence question; this then allows him to consider the possible formalization of convergence characteristics.

For the evaluation of element formulations, as well as being the first step of finite element code validation, the patch test invented by Irons and documented in BAZELEY, CHEUNG, IRONS, ZIENKIEWICZ (1966) has been used by many researchers and commercial code developers. For instance, NAGTEGAAL, NAKAZAWA, TATEISHI (1986) discuss the development of an eight-node shell element based on the assumed strain approach and demonstrate its validity by performing an extensive set of patch test calculations. The concept of patch test is re-examined in a recent paper by TAYLOR, SIMO, ZIENKIEWICZ, CHAN (1986), where the equivalence between the satisfaction of the patch test and the consistency and stability of finite element approximations is discussed. Note that the argument by STUMMEL (1980) seriously questioning the validity of the patch test is countered in this paper.

An important extension of the patch test is proposed in a more recent paper by ZIENKIEWICZ, QU, TAYLOR, NAKAZAWA (1986). Assuming that the consistency of the approximations is satisfied, the test focuses upon the stability of mixed finite elements implied by the Babuska-Brezzi condition [BABUSKA (1973), and BREZZI (1974)]. The procedure involves counting the minimum possible number of active degrees-of-freedom in a patch and comparing this number with the maximum possible number of constraint degrees-of-freedom. If no constraints are imposed on nodal stresses and strains, the mixed iterative solution procedure with continuous interpolation passes the test and is assumed stable. An extension of this stability patch test to the three field formulations of Hu-Washizu type and to plates and shells derived from the Reissner-Mindlin theory is being investigated by ZIENKIEWICZ (1986) and his co-workers.

The relation between the stability patch test and the mathematically derived Babuska-Brezzi condition is also being actively investigated.

Use of the most general mixed variational formulation of the Hu-Washizu type in element development continues to be in the mainstream of research activities. Despite the slight confusion in terminology, a family of simple high performance elements has been developed utilizing, consciously or unconsciously, the mixed method concepts.

Interest in the equal order interpolation for mixed finite element processes is definitely growing. A number of papers and reports have been published not only via this project but also by the research group at Swansea. Also, a number of associated academic research projects have been initiated in the last couple of years. It is anticipated that the number of publications on the utilization of the equal order interpolation mixed method and its iterative solution strategy will increase considerably in the next few years.

2.3 A POSTERIORI ERROR ESTIMATES AND POST-PROCESSING

The methodology used for computing the approximation error in a finite element solution has been improved significantly in the last few years. Also, the adaptive mesh refinement algorithms based on the spatial distribution of error indicators have been developed and applied to a wide range of linear and nonlinear problems. A book on this subject, compiled by Gago, represents present state-of-the-art technology [BABUSKA, ZIENKIEWICZ, GAGO, OLIVEIRA (1986)].

The papers included in the book indicate that a posterior error estimates and adaptive refinement methodologies are well understood mathematically and tested for a wide range of linear elastic problems. However, the computational processes look overly complicated and extensions to nonlinear analysis of solids and structures will need further research and development. Application of the adaptive mesh refinement concept has been demonstrated to be tractable using a relatively simple error indicator for solutions to aerospace flow problems modeled by the compressible Euler equations. Note that the adaptive solution of the compressible Euler equations is the first systematic attempt at extending the technology to nonlinear problems. The results included in the book show the potential advantage of the concept.

A simple algorithm to estimate errors a posteriori is proposed by ZIENKIEWICZ, ZHU (1987). The logic is based on the difference in values for quantities obtained directly within the elements and the same information projected by nodal interpolation functions. The nodal projection techniques used in the mixed, iterative process to recover the nodal strain allow a simple and effective way to calculate errors. This process is relatively easy to implement, in comparison with other seemingly complicated mathematically derived a posteriori error estimate algorithms. Examples shown in the paper indicate the efficiency of the proposed process. However, rigorous mathematical analysis is still to be done to verify the methodology. It is interesting to note that the residual vector calculated at the zeroth iteration of the equal order mixed iterative solution is indeed the Zienkiewicz-Zhu error indicator weight-averaged at nodes.

With triangular elements being employed, efforts to combine automatic mesh-generation and adaptive refinement concepts have been reported. Examples included in ZIENKIEWICZ, ZHU (1987) use this idea. In the application of adaptive mesh refinement to compressible flow problems, a number of papers have been published in which triangular mesh generation methods are discussed in conjunction with local refinement strategy to capture shocks.

PERAIRE, MORGAN, ZIENKIEWICZ (1986) and LOHNER (1986) describe adaptive mesh refinement and de-refinement algorithms designed for triangles and speculate on the applicability of such a concept to three-dimensional computations. The use of automatic mesh generation of triangular and tetrahedral elements has been found to be viable in finite difference flow computations involving unstructured grids. JAMESON (1986) demonstrated possible utilization of this technology for geometrically complex problems.

To summarize then, in the area of a posteriori error estimates, post-processing and adaptive mesh refinement, useful technology has been developed for linear structural analysis and certain nonlinear problems. However, further research and development including extensive numerical experiments will be needed to establish a methodology base for three-dimensional inelastic analyses involving complex loading histories.

2.4 NONLINEAR ANALYSIS OF SOLIDS AND STRUCTURES

Application of finite element methods to nonlinear structural analysis involves increasingly complicated geometrical and material models and pushes currently available supercomputing facilities to their limits. Codes specifically designed for supercomputers have demonstrated such computers' potential. Papers have appeared recently discussing performance improvement of finite element codes on vector and parallel machines utilizing algorithms tailored for a specific computer environment. BENSON, HALLQUIST (1986) discusses the rigid body algorithm implemented in the DYNA code which reduced the amount of computations significantly for explicit finite element time integrations. Implementation of an iterative solution algorithm based on the element-by-element preconditioner in the NIKE code is discussed by HUGHES, FERENCZ, HALLQUIST (1986). The utilization of supercomputers in an engineering environment involving the development of these codes is presented by GOUDREAU, BENSON, HALLQUIST, KAY, ROSINSKY, SACKETT (1986).

Investigations on vectorizability of basic finite element operations continue. For instance, the details of vector-matrix multiplication in an element-by-element manner are discussed, including timing figures, for various finite element models by HAYES, DEVLOO (1986). An algorithm to take full advantage of vector machines in solving a system of ordinary differential equations is proposed by BROWN, HINDMARSH (1986). Iterative algorithms based on the ORTHOMIN method and incomplete factorization are studied by ZYVOLOSKI (1986). It is anticipated that the development of algorithms closely tied to the actual data manipulations and arithmetic operations in computing machines will eventually lead to faster finite element codes not only on supercomputers but also on smaller scalar machines.

Utilization of parallel computing for equation solution is a subject investigated extensively in the last few years. A series of papers by Utku, Melosh and their collaborators looks into the possible parallelization of direct stiffness matrix factorization [UTKO, MELOSH, SALAMA, CHANG (1986); and UTKU, SALAMA, MELOSH (1986)]. The possible utilization of hypercube architecture is studied by NOUROMID, ORTIZ (1986) for the factorization and iterative solution of finite element equations. It is observed in these papers that a simple reduction in the total number of operations does not itself always provide the optimal algorithm for vector and parallel processing. An increasing number of sessions at scientific meetings are now being devoted to discussing this aspect of finite element computations, and extensive literature in this area is being accumulated. However, further research and development still needs to be done before robust algorithms become available for a wide range of engineering applications in order to utilize fully the potential of modern computing machinery.

Notable progress has been made in the last few years in the field of computational plasticity, in particular, design and analysis of integration algorithms for rate-independent plasticity constitutive equations. ORTIZ, SIMO (1986) summarizes the development of such integration algorithms and investigates their accuracy in great detail. The basic idea is to generalize the return mapping algorithm based on the elastic predictor. Application to viscoplastic constitutive equations is also included in this paper. SIMO (1986) extends the results to finite deformation plasticity by developing a simple and efficient finite element algorithm in which elastic deformation of finite amplitude is accommodated.

Approaches for capturing localization due to inelastic material response in global finite element computations have been developed which enable discontinuities to be modeled at the subelement scale. The work by HUGHES, SHAKIE (1986) extends the conventional return mapping algorithm for J_2 flow theory to yield surfaces with corners. This extension enables the effects of localized plastic flow to be captured in a global manner. ORTIZ, LEROY (1986) proposes an algorithm which allows shear bands to generate inside a finite element. The numerical results indicate the potential of the method for capturing local failure of structures without excessive mesh refinement. Methods for bringing in local failure modes in finite elements to capture

localization effects under strain softening are discussed by WILLAM, SOBH, STURE (1986). A survey of the finite element technology for capturing localized failure modes is given by NEEDLEMAN (1986). This is a relatively new field and further work will be needed before localized microscopic material responses due to embedded singularities in large-scale structural systems can be calculated effectively.

2.5 CONCLUDING REMARKS

In the theoretical aspects of finite element development, the utilization of the mixed variational principle has been and continues to be the main thrust of research and development work. This approach not only provides tools to improve the performance of elements but also leads to a deeper insight on the solution algorithms for linear and nonlinear problems. The mixed iterative methodology developed under the HOST contract takes full advantage of these modern theoretical developments. Also, new ideas demonstrated in the MHOST program have attracted significant academic research interest in the computational mechanics community.

In the application and computational aspects of finite elements, progress made in the last few years has not yet been fully incorporated into the MHOST code development. The information available in the literature indicates that further development to utilize modern algorithms and coding technology would enhance the performance of the MHOST code even more significantly.

3.0 GLOBAL SOLUTION STRATEGY AND ELEMENT FORMULATION

3.1 INTRODUCTION

This section summarizes the technology developed and implemented in the MHOST program during Task VB.

The mixed variational formulation of Hu-Washizu type [HU (1955), and WASHIZU (1955, 1974)] is used as a driving mechanism to derive the iterative solution algorithms. A system of algebraic equations is generated, including the effects of the stress stiffening and the centrifugal mass terms in conjunction with the dynamic transient effects in a semi-discrete manner. The fully-discretized version of the finite element equation system is included in this report, with the Newmark family of algorithms used for temporal discretization. As demonstrated in ZIENKIEWICZ, LI, NAKAZAWA (1986), other time integration algorithms can be utilized to generate recursive forms for transient analyses.

The implementation of iterative solution algorithms for the mixed finite element equations is briefly discussed in this section. A comparison of options made available in the MHOST code indicates that the secant version of the Davidon rank-one quasi-Newton update performs most reliably, except for a class of ill-conditioned problems.

The updated Lagrangian formulation is used to facilitate large displacement effects. The inclusion of finite strain effects provides an experimental capability in the latest version of the MHOST code. A subsection is devoted to this development.

Element formulations based on the selectively reduced integration and the assumed strain approaches are investigated. In the mixed iterative solution framework, element formulations applicable to anisotropic material response with rate independent deviatoric plasticity are identified as requiring further investigation.

The subelement method is extended to handle inelastic response inside subelement regions. The validation cases included in this context indicate the performance of this new approach in capturing local inelastic responses around embedded singularities.

3.2 SEMIDISCRETE FINITE ELEMENT EQUATIONS AND TEMPORAL DISCRETIZATION

The finite element equations of dynamic equilibrium for a deformable body can be written in terms of the nodal acceleration vector $\mathbf{a}$, the nodal velocity vector $\mathbf{v}$ and the nodal stress vector $\mathbf{s}$ as follows:

$$\mathbf{M}\,\mathbf{a} + \mathbf{C}\,\mathbf{v} + \mathbf{B}\,\mathbf{s} = \mathbf{F}, \tag{1}$$

where $\mathbf{M}$ is the mass matrix defined by

$$\mathbf{M} = \rho \int_{\Omega} \mathbf{N}^T \mathbf{N} \, dx \tag{2}$$

with ρ and $\mathbf{N}$ being the material density and the vector of interpolation functions respectively. The damping matrix $\mathbf{C}$ may be defined as a sum of mass and stiffness matrices, $\mathbf{M}$ and $\mathbf{K}$, such that

$$\mathbf{C} = P_1 \mathbf{M} + P_2 \mathbf{K}, \tag{3}$$

with P_1 and P_2 being preassigned constants representing the effects of viscous and structural damping respectively. Symbolically, the stiffness matrix can be written by

$$\mathbf{K} = \int_{\Omega} \nabla \mathbf{N}^T \mathbf{D} \, \nabla \mathbf{N} \, dx , \tag{4}$$

with ∇ being the gradient operator and $\mathbf{D}$ the material modulus. The third term in Equation (1) represents the internal energy, with the $\mathbf{B}$ matrix being the discrete gradient operator defined in the finite element approximation subspace such that

$$\mathbf{B} = \int_{\Omega} \nabla \mathbf{N}^T \mathbf{N} \, dx. \tag{5}$$

Here an equal order interpolation using the same basis functions is assumed for the acceleration, velocity, displacement, and stress. The nodally interpolated strain is recovered via

$$\mathbf{e} = \mathbf{G}^{-1} \mathbf{B}^T \mathbf{u}, \tag{6}$$

where $\mathbf{G}$ is the diagonalized gramm matrix whose Ith diagonal entry is calculated by

$$G_I = \sum_{J=1}^{N_P} \int_{\Omega} N_I \, N_J \, dx, \tag{7}$$

with N_P being the total number of nodes in a mesh. The nodal stress state is recovered by

$$\mathbf{s} = \mathbf{D} \, \mathbf{e}. \tag{8}$$

Note that all the integrations indicated in the above equations are evaluated approximately using numerical quadrature. The particular choice of numerical integration rule is discussed in the subsection on element formulation.

Next, an abstract iterative process is constructed for the semi-discrete Equations (1) by means of displacement preconditioning. The approximation of internal energy by the product of stiffness matrix $\mathbf{K}$ and total displacement vector $\mathbf{u}$ leads to the recursive expression

$$\mathbf{M}\,\mathbf{a}_{i+1} + \mathbf{C}\,\mathbf{v}_{i+1} + \mathbf{K}\,\mathbf{u}_{i+1} = \mathbf{F} - (\mathbf{B}\,\mathbf{s}_i - \mathbf{K}\,\mathbf{u}_i), \tag{9}$$

with subscripts denoting the iteration counter. For linear elastic problems, the displacement converges linearly given an appropriate initial condition such as $\mathbf{u}_0 = 0$.

Note that the strain projection procedure and the stress recovery operation, Equations (6) and (8), are executed every time the displacement vector is updated.

The fully discretized system of equations is derived for the mixed iterative solution by introducing the temporal approximation. For the sake of simplicity and clarity, the Newmark family of algorithms is introduced in a finite difference fashion, e.g., HUGHES (1984), such that dynamic equilibrium is satisfied at time $t + \Delta t$ as follows:

$$\mathbf{M}\,\mathbf{a}^{t+\Delta t} + \mathbf{C}\,\mathbf{v}^{t+\Delta t} + \mathbf{B}\,\mathbf{s}^{t+\Delta t} = \mathbf{F}^{t+\Delta t}. \tag{10}$$

This then leads to a time discrete displacement preconditioning

$$\mathbf{M}\,\mathbf{a}_{i+1}^{t+\Delta t} + \mathbf{C}\,\mathbf{v}_{i+1}^{t+\Delta t} + \mathbf{K}\,\mathbf{u}_{i+1}^{t+\Delta t} = \mathbf{F}^{t+\Delta t} - (\mathbf{B}\,\mathbf{s}_i^{t+\Delta t} - \mathbf{K}\,\mathbf{u}_i^{t+\Delta t}), \tag{11}$$

with the updates for displacement and velocity given by

$$\mathbf{u}_i^{t+\Delta t} = \mathbf{u}^t + \Delta t\ \mathbf{v}^t + \frac{\Delta t^2}{2}\left\{(1 - 2\beta)\ \mathbf{a}^t + 2\beta\,\mathbf{a}_i^{t+\Delta t}\right\}, \tag{12}$$

$$\mathbf{v}_i^{t+\Delta t} = \mathbf{v}^t + \Delta t\ \left\{(1 - \gamma)\ \mathbf{a}^t + \gamma\,\mathbf{a}_i^{t+\Delta t}\right\}. \tag{13}$$

With the aid of

$$\Delta\mathbf{u}_i^{t+\Delta t} = \mathbf{u}_i^{t+\Delta t} - \mathbf{u}^t \tag{14}$$

and

$$\delta\mathbf{u}_i^{t+\Delta t} = \Delta\mathbf{u}_{i+1}^{t+\Delta t} - \Delta\mathbf{u}_i^{t+\Delta t}, \tag{15}$$

a recursive form is obtained as follows:

$$\left\{ \left(\frac{1}{\beta\Delta t^2}\right) \mathbf{M} + \left(\frac{\gamma}{\beta\Delta t}\right) \mathbf{C} + \mathbf{K} \right\} \delta \mathbf{u}_i^{t+\Delta t}$$

$$= \mathbf{F}^{t+\Delta t} - \left[\mathbf{B}\, \mathbf{s}_i^{t+\Delta t} + \left\{ \left(\frac{1}{\beta\Delta t^2}\right) \mathbf{M} + \left(\frac{\gamma}{\beta\Delta t}\right) \mathbf{C} \right\} \Delta \mathbf{u}_i^{t+\Delta t} \right]$$

$$+ \left(\frac{\gamma}{\beta} - 1\right) \mathbf{C}\, \mathbf{v}^t + \left(\frac{\gamma}{2\beta} - 1\right) \Delta t\, \mathbf{C}\, \mathbf{a}^t$$

$$+ \left(\frac{1}{\beta\Delta t}\right) \mathbf{M}\, \mathbf{v}^t + \left(\frac{1}{2\beta} - 1\right) \mathbf{M}\, \mathbf{a}^t , \tag{16}$$

where the incremental displacement $\Delta \mathbf{u}_{i+1}^{t+\Delta t}$ is updated by

$$\Delta \mathbf{u}_{i+1}^{t+\Delta t} = \Delta \mathbf{u}_i^{t+\Delta t} + \delta \mathbf{u}_i^{t+\Delta t} \tag{17}$$

and the incremental strain is recovered at each node by

$$\Delta \mathbf{e}_i^{t+\Delta t} = \mathbf{G}^{-1}\, \mathbf{B}^T\, \Delta \mathbf{u}_i^{t+\Delta t} . \tag{18}$$

In a general setting of history dependent inelastic constitutive integration, the stress recovery process is written as

$$\mathbf{s}_{i+1}^{t+\Delta t} = \mathbf{s}^t + \int_0^{\Delta \mathbf{e}_i^{t+\Delta t}} \mathbf{s}\, d\, \mathbf{e} \tag{19}$$

which is fed into the equilibrium iteration defined by Equation (16).

The computational effort in the above iterative process for direct time integration of the discrete equations of motion involves assembly of the element operator matrices which appear on the left-hand side of Equation (16). This requires exactly the same amount of effort as to solve the problem by the conventional displacement method. Additional computations required for the mixed solution involve a few back substitutions and strain and stress recovery at nodes, computations which are relatively inexpensive compared to matrix assembly and factorization. This additional computational cost would vanish when the scheme is applied to nonlinear problems in which matrix assembly and factorization or back substitution need to be performed repeatedly no matter which finite element method is used to drive the solution. Therefore, the

seemingly complicated derivation of the mixed iterative solution scheme does not increase the computational effort in comparison with the displacement formulation. Thus, the advantages of equal order interpolation of displacement, strain and stress can be fully utilized without fear of central processing unit (CPU) time penalties.

With particular attention to turbo machinery blades and other rotating structures, the stiffness matrix can be modified to include the effects of the stress stiffening and the centrifugal mass terms. These results are based on linearized models of the large displacement and corresponding follower force equations under a given angular velocity.

The centrifugal load vector is generated by integrating the body force

$$\mathbf{F}_0 = \int_{\Omega} \mathbf{N}^T \rho\omega^2 \, \mathbf{r}(\mathbf{x}) \, d\mathbf{x} , \tag{20}$$

with ω being the angular speed and $\mathbf{r}$ the vector distance between a point and the axis of rotation. Under the centrifugal loading given above, the mixed iterative algorithm generates a certain stress field represented by the nodal stress vector $\mathbf{s}_0$ such that the discrete equilibrium equation

$$\mathbf{B}\,\mathbf{s}_0 = \mathbf{F}_0 \tag{21}$$

is satisfied. Our interest here is to calculate the linearized response of the structure under an initial state of stress given by $\mathbf{s}_0$. If these initial stress terms are taken into account, the equilibrium equation system is modified (excluding the damping term) to

$$\mathbf{M}\,\mathbf{a} + \mathbf{K}_G^0\,\mathbf{u} + \mathbf{B}^T\mathbf{B} = \mathbf{F} , \tag{22}$$

where $\mathbf{K}_G^0$ is the geometric stiffness term associated with the initial stress field $\mathbf{s}_0$ and is given by

$$\mathbf{K}_G^0 = \int_{\Omega} \nabla\mathbf{N}^T \, \mathbf{s}^0 \, \nabla\mathbf{N} \, d\mathbf{x} . \tag{23}$$

Note that Equation (22) is a general expression for the linearized response of structural systems under a prescribed initial stress field.

When this term, i.e., $\mathbf{K}_G^0\mathbf{u}$, is included in the mixed iterative computations, the abstract recursive form, Equation (9), becomes:

$$\mathbf{M}\,\mathbf{a}_{i+1} + (\mathbf{K}_G^0 + \mathbf{K})\,\mathbf{u}_{i+1} = \mathbf{F} - (\mathbf{B}\,\mathbf{s}_i - (\mathbf{K}_G^0 + \mathbf{K})\,\mathbf{u}_i), \tag{24}$$

or in terms of displacement update

$$(\mathbf{K}_G^0 + \mathbf{K})\ \Delta\mathbf{u}_i = \mathbf{F} - (\mathbf{B}\,\mathbf{s}_i - \mathbf{K}_G^0\ \mathbf{u}_i), \tag{25}$$

with

$$\mathbf{u}_{i+1} = \mathbf{u}_i + \Delta\mathbf{u}_i\ .$$

In the residual force calculations, the initial stress matrix needs to be evaluated repeatedly with the stress field calculated at the beginning of the increment.

The additional force due to the relative motion from the equilibrium position, referred to as the centrifugal mass term, is also added to the equilibrium equation system resulting in

$$\mathbf{M}\,\mathbf{a} + (\mathbf{K}_G^0 - \mathbf{M}_c)\ \mathbf{u} + \mathbf{B}\,\mathbf{s} = \mathbf{F}\ , \tag{26}$$

where $\mathbf{M}_c$ is the centrifugal mass matrix defined by

$$\mathbf{M}_c = \int_\Omega \rho\omega^2\ \mathbf{N}^T\,\mathbf{L}\,\mathbf{N}\ d\mathbf{x}\ , \tag{27}$$

with $\mathbf{L}$ being a matrix based upon the components of the unit vector $\mathbf{m}$ parallel to the axis of rotation. $\mathbf{L}$ is given by

$$\mathbf{L} = \begin{vmatrix} m_2^2+m_3^2 & -m_1m_2 & -m_3m_1 \\ -m_1m_2 & m_3^2+m_1^2 & -m_2m_3 \\ -m_3m_1 & -m_2m_3 & m_1^2+m_2^2 \end{vmatrix}\ . \tag{28}$$

When this term is activated in the quasi-static and transient dynamic computations, an additional correction of the residual vector calculation is made by replacing $\mathbf{K}_G^0$ with $(\mathbf{K}_G^0 - \mathbf{M}_c)$.

Typically, these optional terms are activated for the vibration analysis of rotating structures by extracting the modes of the eigenvalue problem

$$\left\{\mathbf{M} - \lambda(\mathbf{K}_G^0 - \mathbf{M}_c + \mathbf{K})\right\}\ \mathbf{x} = 0. \tag{29}$$

In the modal analysis, the displacement preconditioner is assumed to represent the structural stiffness. However, the stress values used in the evaluation of initial stress terms are calculated by the mixed iterative method. Thus, a more accurate stress field is generated than via the conventional displacement method. Hence, the solution of Equation (29) is expected to be somewhat more accurate than that associated with the displacement method approach.

For details of derivations of initial stress and centrifugal mass matrices and fully worked out examples, see THOMAS, MOTA SOARES (1973) and RAWTANI, DOKAINISH (1971).

In summary then, Equation (16) represents the recursive form of the basic time discrete displacement preconditioning as given by Equation (11); furthermore, Equation (11) itself is a discretized form of the original basic equation of dynamic equilibrium as given by Equation (1). The bottom line, however, is that the sequence of computations for the basic equation set is given by the order of Equations (16) through (19). For centrifugal load effects, Equations (24) and (25) replace Equations (16) and (17) and Equations (20) and (23) are also added.

3.3 GLOBAL SOLUTION ALGORITHMS

In the present implementation of the mixed iterative solution procedures, the displacement stiffness equations need to be assembled and factorized. To enhance the efficiency of the MHOST code, a new profile solver algorithm has been developed to replace the constant bandwidth Crout decomposition algorithm. The implementation of this new profile solver is based on code published by TAYLOR (1985). Examples presented in that paper include both symmetric and nonsymmetric cases using Crout decomposition. Implementation of the profile solver into the MHOST code excludes a nonsymmetric capability in order to gain maximum efficiency. The profile storage of the global stiffness equations reduces memory requirements as well as time required for factorization. Additional computational overhead is required to prepare the elimination table for a stiffness matrix stored in profile form. A table comparing the performance of these solvers is included in Section 4.4.1.

In the quasi-static computations, a series of options to accelerate the rate of convergence for nonlinear iterations has been made operational with the new profile solver capability. These options are as follows: the modified Newton method, the quasi-Newton method of inverse BFGS update, the secant Newton implementation of Davidon rank-one quasi-Newton update, the conjugate gradient method, and the line search method. The spherical path version of the arc length method incorporating modified Newton iteration is also now available with the profile solver capability. For details of the implementation of these numerical processes in the mixed iterative solution framework, see the third year progress report [NAKAZAWA (1986)].

The eigenvalue extraction procedure implemented into the MHOST code is based on the subspace iteration approach documented by BATHE, WILSON (1976). In this process, the large eigenproblem of structural systems is mapped into a subspace of finite dimensions and Jacobi iteration is performed to solve the small eigenproblem set in the subspaces. This eigenvalue extraction procedure

is used to compute the natural frequency and vibration mode of unstressed and prestressed structures as well as the buckling analysis of prestressed structures undergoing elastic or inelastic deformation of infinitesimal or finite amplitude.

Note here that in the eigenvalue extraction, the standard displacement stiffness matrix is used to represent the response of structural systems. However, in buckling and modal analyses with prestress, the improvement of the stress field generally improves the quality of the solution considerably. The utilization of mixed stress interpolation in the eigenvalue analysis can be viewed as equivalent to a perturbed eigenvalue problem in which the effect of the independent stress approximation is regarded as the perturbation to the displacement finite element system. It is anticipated that an algorithm proposed by SIMO (1985) and implemented for the probabilistic finite element code at MARC may be usable for eigenvalue extraction of mixed systems of finite element equations.

3.4 LARGE DISPLACEMENT ANALYSIS

In this section, the large deformation algorithm implemented in the mixed iterative method is described. The formulation utilizes an updated Lagrangian mesh approach. The choice of deformation and stress measures in finite deformation analysis depends primarily on the class of material involved, along with the necessity that the measures are objective (invariant) for rigid body motions. For elastic-plastic behavior where the response depends primarily on the current state of stress, a Cauchy stress and rate-of-deformation (i.e., strain rate) constitutive formulation is frequently most convenient.

Beyond the choice of a Lagrangian mesh description, the formulation can be further simplified by evaluating the equations of motion at the current (deformed) configuration. This is achieved by continually updating the mesh geometry to the current state. Utilizing an updated geometry results in simplification because all matrix expressions take the same form as in small deformation theory. The only additional quantities needed are deformation gradients and rotation tensors evaluated at nodes, along with follower force matrices. This formulation is referred to as the updated Lagrangian approach in the literature.

The updated Lagrangian algorithm for large deformation problems is essentially the same as that for nonlinear small deformation problems, with the exception that all tensors and integrals are evaluated with respect to the current configuration. The updated Lagrangian algorithm presented in this section involves nodal coordinates being updated continuously and deformation gradients being evaluated at nodes.

Table 1 presents a summary of the algorithm for an increment. All new terms in this table are defined in the Nomenclature section. Following initialization, the process is repeated iteratively until equilibrium has been satisfied.

Table 1 Updated Lagrangian Algorithm

Initialization:

$$\mathbf{u}^i = \mathbf{u}^{i-1} \qquad [\sigma]^i = [\sigma]^{i-1} \qquad \mathbf{R}^i = \mathbf{F}_E^i$$

Equation Formulation and Displacement Solution:

$$\Delta \mathbf{u}^i = (\mathbf{K}^i)^{-1}\, \mathbf{R}^i$$

Update Geometry:

$$\mathbf{x}^{i+1} = \mathbf{x}^i + s^i\, \Delta \mathbf{u}^i \qquad \mathbf{F}_{rel}^{i+1/2} = \mathbf{I} + s^i\, \nabla\left(\tfrac{1}{2}\, \Delta \mathbf{u}^i\right)$$

$$\mathbf{u}^{i+1} = \mathbf{u}^i + s^i\, \Delta \mathbf{u}^i \qquad \mathbf{F}_{rel}^{i+1} = \mathbf{I} + s^i\, \nabla(\Delta \mathbf{u}^i)$$

$$\mathbf{F}^{i+1/2} = \mathbf{F}_{rel}^{i+1/2}\, \mathbf{F}^i \qquad \mathbf{R}^{i+1/2} = \mathbf{F}^{i+1/2}\, (\mathbf{U}^{i+1/2})^{-1}$$

$$\mathbf{F}^{i+1} = \mathbf{F}_{rel}^{i+1}\, \mathbf{F}^i \qquad \mathbf{R}^{i+1} = \mathbf{F}^{i+1}\, (\mathbf{U}^{i+1})^{-1}$$

Strain Projection:

Large Strain

$$\Delta[\epsilon]^{i+1} = (\mathbf{CS}^{i+1})^{-T}\, \mathbf{B}^{i+1}\, s^i\, \Delta \mathbf{u}^i$$

Small Strain

$$\Delta[\epsilon]^{i+1} = (\mathbf{CS}^{i})^{-T}\, \mathbf{B}^{i}\, s^i\, \Delta \mathbf{u}^i$$

Stress Recovery:

$$[\sigma]_R^{i+1} = \mathbf{D}_R^{i+1}\, (\mathbf{ROT}^{i+1/2})^T\, \Delta[\epsilon]^{i+1}\, \mathbf{ROT}^{i+1/2} + [\sigma]^i$$

Table 1 Updated Lagrangian Algorithm (continued)

Rotate Back to Global System:

$$[\sigma]^{i+1} = \mathbf{ROT}^{i+1}[\sigma]_R^{i+1}(\mathbf{ROT}^{i+1})^T \qquad [\epsilon]_{PL}^{i+1} = \mathbf{ROT}^{i+1}[\epsilon]_{PL_R}^{i+1}(\mathbf{ROT}^{i+1})^T$$

$$\mathbf{D}^{i+1} = \mathbf{ROT}^{i+1}\ \mathbf{D}_R^{i+1}\ (\mathbf{ROT}^{i+1})^T \qquad [\alpha]^{i+1} = \mathbf{ROT}^{i+1}[\alpha]_R^{i+1}(\mathbf{ROT}^{i+1})^T$$

Form Residual:

$$\mathbf{R}^{i+1} = \int_{\Omega^{i+1}} (\mathbf{N}^{i+1})^T\ \mathbf{f}^{i+1}\ \mathbf{N}^{i+1}\ dx^{i+1}$$

$$+ \int_{\partial\Omega^{i+1}} (\mathbf{N}^{i+1})^T\ \mathbf{h}^{i+1}\ \mathbf{N}^{i+1}\ dS^{i+1}$$

$$- (\mathbf{B}^{i+1})^T [\sigma]^{i+1}$$

If converged, exit; otherwise update displacements via line search or displacement solution and repeat.

In the finite displacement calculations, the stiffness array is assembled in the following manner and repeatedly updated in the iteration loop unless another iteration process (modified-Newton, quasi-Newton, or secant-Newton option) is specified. Note that the stiffness matrix does not correspond to the classical Newton method in the mixed iterative solution framework because of the independent C^0-continuous stress interpolation functions. Here, $\bar{\mathbf{B}}$ is the conventional strain displacement matrix.

$$\mathbf{K}^i = \int_{\Omega^i} \bar{\mathbf{B}}^T(\mathbf{x}^i)\ \mathbf{D}_T^i\ \bar{\mathbf{B}}(\mathbf{x}^i)\ d\mathbf{x}^i$$

Tangent stiffness matrix

$$+ \int_{\Omega^i} \bar{\mathbf{B}}^T(\mathbf{x}^i)[\sigma]^i\bar{\mathbf{B}}(\mathbf{x}^i)\ d\mathbf{x}^i$$

Initial stress matrix

$$- \int_{\xi} \mathbf{N}^T(\mathbf{x}^i)\ \mathbf{f}^{i+1}\ \mathbf{N}(\mathbf{x}^i)\ \mathbf{J}^i_{,\xi}\ (\mathbf{J}^i)^{-1}\ d\xi$$

Body force follower force due to volume change

(30)

$$- \int_{\partial\xi} \mathbf{N}^T(\mathbf{x}^i)\ \mathbf{h}^{i+1}\ \mathbf{N}(\mathbf{x}^i)\ \mathbf{J}^i_{,\xi}\ (\mathbf{J}^i)^{-1}\ d\xi$$

Surface traction follower force due to surface area change

$$- \int_{\Omega^i} [\nabla\mathbf{N}^T(\mathbf{x}^i)\ \mathbf{f}^{i+1}\mathbf{N}(\mathbf{x}^i) + \mathbf{N}^T(\mathbf{x}^i)\ \mathbf{f}^{i+1}\nabla\mathbf{N}(\mathbf{x}^i)]\ d\mathbf{x}^i$$

Body force follower force due to rotation

$$- \int_{\partial\Omega^i} [\nabla\mathbf{N}^T(\mathbf{x}^i)\ \mathbf{h}^{i+1}\mathbf{N}(\mathbf{x}^i) + \mathbf{N}^T(\mathbf{x}^i)\ \mathbf{h}^{i+1}\nabla\mathbf{N}(\mathbf{x}^i)]\ dS$$

Surface traction follower force due to rotation

Whenever the stiffness matrix is reformulated in an updated Lagrangian algorithm, the shape functions, derivatives of the shape functions and determinants of Jacobians are evaluated at the nodal coordinates of the current configuration. In addition, the material and stress matrices used are those computed in the immediately preceding iteration.

4.0 COMPUTER PROGRAM DEVELOPMENT AND VALIDATION

4.1 INTRODUCTION

Version 4 of the MHOST code consists of over 47,000 lines of FORTRAN source statements including extensive comments. The concept of multiple-analysis drivers has been used to maintain the quality and efficiency of the code. A brief discussion of the architecture of the code is presented in this report.

Note that the multiple driver strategy has kept the code usable for well tested capabilities, while new options and enhancements of existing features were being developed and tested. Also, such a strategy has helped to keep the code readable since the number of conditional statements is minimized. In order to use this code effectively for production purposes in engineering environments, further streamlining of the code would be needed to improve the performance of this finite element package.

The user interface has been enhanced to deal with numerous algorithmic options added to Version 4 of this code. A subsection briefly summarizes the program features and user commands.

All the development work has been carried out on a PRIME 9955 at MARC Analysis Research Corporation. The PRIME FORTRAN 77 compiler is employed without extensive utilization of extensions to ANSI standard. Versions for VAX/VMS, IBM/CMS and CRAY/COS environments have been created and tested using their FORTRAN 77 compilers. The utilization of FORTRAN 77 features which are not supported by the previous FORTRAN standard have made the new code incompatible with the old FORTRAN compilers.

A profile solver approach has replaced the constant bandwidth Crout decomposition routines. The new solution package improves the efficiency of the code significantly in terms of both core storage and computing speed. A large portion of the MHOST code has been rewritten to take advantage of this new solver capability, including the quasi-static analysis, eigenvalue extraction and transient time integration subsystems. The out-of-core frontal solution subsystem remains unchanged and may be employed for large-scale small deformation quasi-static calculations.

4.2 COMPUTER CODE ARCHITECTURE

The architecture of the MHOST code is schematically shown in Figure 1. The execution supervisor routine (SUBROUTINE HOST) controls a multiple number of analysis modules in a consistent manner. In Version 4 of the MHOST code, a pair of subroutines has been added to check the consistency of the Parameter Data and to generate internal flags for the selection of analysis modules. The objective here is to avoid combining features of the program package not intended by the developers to be combined.

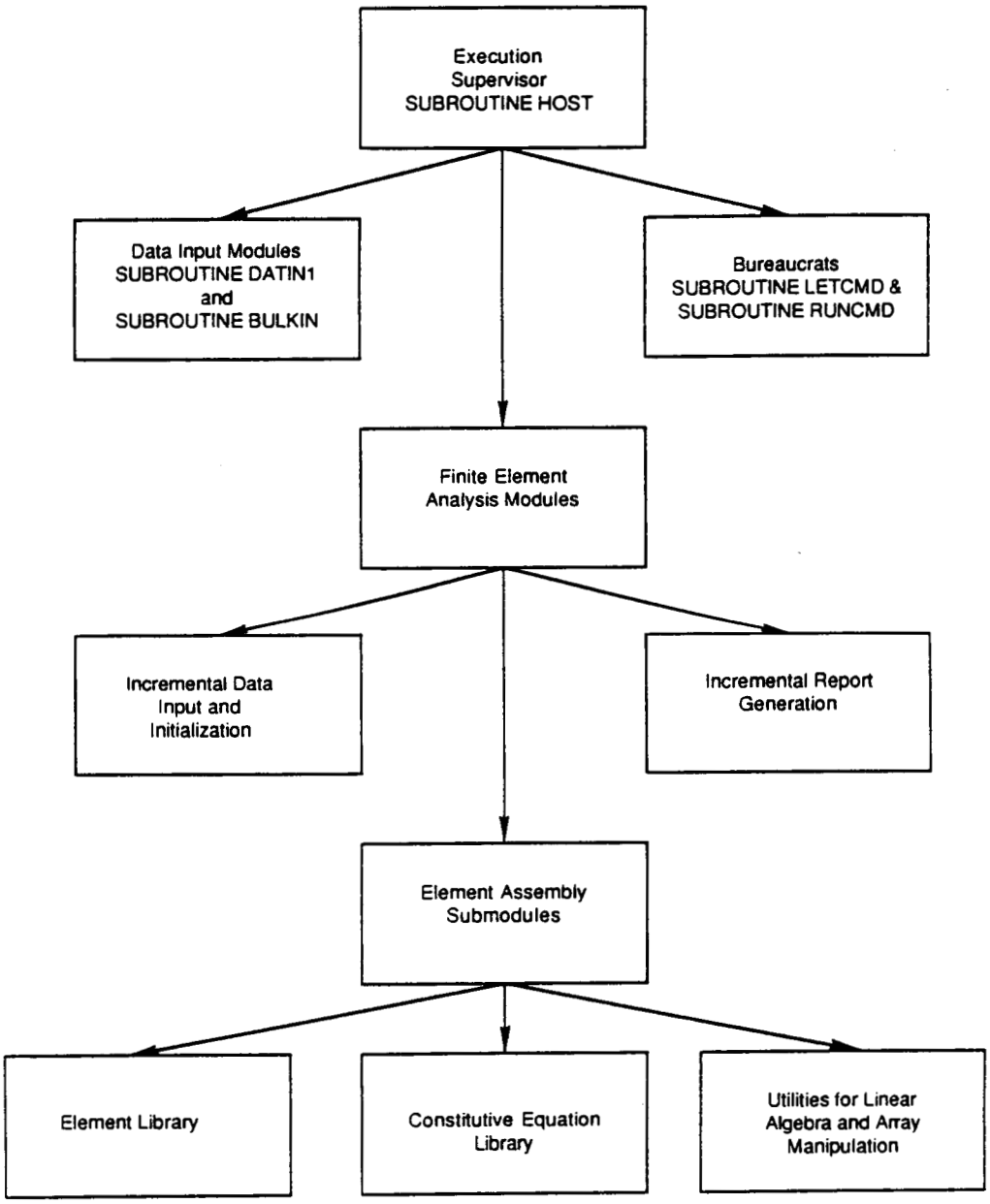

Figure 1 Architecture of the MHOST Code Version 4.2

The analysis modules provide the control structure for the incremental iterative algorithms implemented in the MHOST code. The source program with comments is designed to serve as the schematic flow chart of the computational process.

The schematic flow of the element and nodal data manipulations is coded in the element assembly submodules which are entered from the analysis modules. The element assembly submodules perform operations independent of element type and constitutive model. The assumptions introduced in the mechanics aspects of the formulations are explicitly coded at this level. These submodules call the librarian routines for elements and constitutive models.

The element librarian subprogram (SUBROUTINE DERIV) generates quantities unique to the element used in an analysis. The MHOST code uses for the most part the standard finite element matrix notation, as in ZIENKIEWICZ (1977). The element specific information returned from the librarian subprogram is the strain-displacement array referred to as the $\bar{\mathbf{B}}$ matrix in previous subsections.

The constitutive equation librarian subprogram (SUBROUTINE STRESS and BMSTRS) is designed to accommodate the nodal storage of stress and strain values. The STRESS subroutine sets up the loop over the points at which constitutive equations are evaluated. The current implementation is a nested double loop with the outer loop being over the nodes and the inner loop over the integration layers through the thickness. Note that the conventional displacement method can be recovered by restructuring this loop in conjunction with a few minor modifications in the core allocation for stresses and strains.

The librarian subprogram calls the constitutive equation package (SUBROUTINE NODSTR) from which individual subprograms for initial strains, stress recovery and material tangent are accessed. The librarian subprogram also controls the pre-integration of stresses, strains and material tangent over thickness for the shell element.

The evaluation of the constitutive equations is one of the most costly operations in the nonlinear finite element computations. An attempt has been made to minimize the execution of this process during the incremental iterative analysis, typically once every iteration during the recovery of the residual vector. At the beginning of each increment, this process may be executed to evaluate the material tangent as well as the contribution of initial strain terms which are often necessary for proper displacement pre-conditioning.

Except for a small amount of information related to the convergence of the iterative solution, all report generation is performed at the end of an increment. Optionally, post-processing and restart files are written at the end of user-specified increments. Generic reporting subprograms are called from analysis modules inside the loop over the increments.

A brief description of major subprograms is provided below.

Execution Supervisor

MAIN PROGRAM - declares the work space in blank common as an integer array. Also defines system parameters which are machine independent. Then passes control to the actual execution supervisor SUBROUTINE HOST.

SUBROUTINE HOST - controls the sequence of execution of analysis modules. First, this routine executes the control parameter data reader SUBROUTINE DATIN1 and checks for consistency by entering SUBROUTINE LETCMD and RUNCMD. The current structure of the code allows certain combinations of two analysis modules to be executed sequentially. Analysis modules called from the execution supervisor are as follows:

SUBROUTINE STATIC for a quasi-static incremental iterative solution.

SUBROUTINE DYNAMT for a transient time integration of the dynamic equilibrium equation system in an incremental-iterative manner.

SUBROUTINE MODAL for eigenvalue extraction in vibration mode analysis. This subsystem may be executed after a quasi-static analysis for modal analysis of prestressed structures.

SUBROUTINE BUCKLE for eigenvalue extraction in buckling load calculations. This subsystem is executable only after a quasi-static analysis.

SUBROUTINE FRONTS for a quasi-static incremental iterative solution by the out-of-core frontal solution procedure. Note that certain options are not available in this subsystem.

SUBROUTINE SUPER for a linear dynamic response calculation by the method of mode superposition.

Input Data Reader

There are three major subprograms:

SUBROUTINE DATIN1 - Reads and interprets the parameter data input called by the execution supervisor. All the default values for control variables are set in this routine.

SUBROUTINE BULKIN - Reads and interprets the finite element model definition data and prints the mesh and loading data for the initial increment (number 0). The bulk data reader is entered before the execution of analysis modules. This subroutine utilizes the following lower level routines:

SUBROUTINE INITI1 for the memory allocation of integer work space in the blank common to store nodal and element data.

SUBROUTINE DATIN2 for the model data input.

SUBROUTINE DATOU1 for reporting the model definition data.

SUBROUTINE CHKELM for the detection of clockwise element connectivity which results in a negative Jacobian matrix. This routine automatically corrects the connectivity table to a counterclockwise direction.

SUBROUTINE SUBDIV for memory allocation of subelement mesh data and automatic mesh generation of subelements.

SUBROUTINE INCRIN - Reads and interprets the loading and constraint data for each increment. This routine is invoked by individual analysis modules from inside the loop over the increments.

SUBROUTINE DATIN3 - A small subset of the bulk data reader SUBROUTINE DATIN1, is used for actual operations including initialization of arrays at the beginning of an increment.

Algebraic Operations Subsystem

There are three packages of routines for the profile solver, frontal solver and eigenvalue extraction. The profile solution package consists of:

SUBROUTINE COMPRO - Sets up the integer array for the profile of the global stiffness equations to be stored in a profile form.

SUBROUTINE ASSEM5 - Assembles the element stiffness equations into the global equation system stored in a profile form.

SUBROUTINE SOLUT1 - Controls the iterative solution processes including the vector update required for the quasi- and secant-Newton iterations.

SUBROUTINE DECOMP - Factorizes the global stiffness equations stored into a profile form.

SUBROUTINE SOLVER - Performs the back substitution and generates the update vector for the incremental displacement.

The frontal solution package consists of:

SUBROUTINE FRONTW - Estimates the front matrix size to be accommodated in the core memory.

SUBROUTINE INTFR - Allocates memory for the work space required for the frontal solution.

SUBROUTINE PRFRNT - Sets up the elimination table for the frontal solution.

SUBROUTINE FRONTF - Assembles and factorizes the global stiffness equations simultaneously.

SUBROUTINE FRONTB - Performs the back substitution and generates the updates for the displacement vector.

SUBROUTINE FRONTR - Controls the iterative solution processes including the vector update required for the quasi- and secant-Newton iterations. Calls SUBROUTINE FRONTB for the incremental displacement update vector.

SUBROUTINE VDSKIO - Controls the data stream stored in the in-core buffer area and the actual out-of-core storage devices.

The eigenvalue analysis package consists of:

SUBROUTINE EIGENV - Controls execution of the eigenvalue extraction subsystem.

SUBROUTINE INIMOP - Initializes the array for eigenvectors.

SUBROUTINE SUBSPC - Performs the subspace iteration and generates a specified number of eigenvalues and eigenvectors.

SUBROUTINE JACOBI - Solves the eigenvalue problem in the subspace by Jacobi iteration.

There are a number of subprograms used commonly by the Algebraic Operations Subsystem:

SUBROUTINE STRUCT - Controls memory allocation for global algebraic manipulations at the beginning of every increment.

SUBROUTINE INITI2 - Allocates memory required for storage of the global stiffness matrix and other vectors necessary in the linear algebraic manipulation of the finite element equations.

SUBROUTINE LINESR - Calculates the search distance when the line search option is turned on.

Element Assembly Submodules

These are subprograms constructing vectors and matrices appearing in the algorithmic description of the mixed iterative process discussed in previous subsections.

SUBROUTINE ASSEM1 - Assembles the displacement stiffness matrix for preconditioning purposes. All the options for kinematic and constitutive assumptions are tested in this module.

SUBROUTINE ASSEM2 - Assembles the coefficient matrix for the transient time integration by the Newmark family of algorithms. This routine is evolved from SUBROUTINE ASSEM1 and contains all the options.

SUBROUTINE ASSEM3 - Assembles the coefficient matrix for the quasi-static analysis using the frontal solution subsystem. Large displacement, stress stiffening and centrifugal mass terms are not available in this package.

SUBROUTINE ASSEM4 - Calculates the nodal strain and recovers the residual vector in a mixed form. The subelement solution package is entered from this subprogram.

Element Loop Structure and Library Routines

In the element assembly submodules, element arrays are generated in loops over the elements. The protocol for accessing the element library involves a sequence of subroutine calls as follows:

SUBROUTINE ELVULV - Sets up the current element parameters (see Table 2 for variables and values) from the element library table.

SUBROUTINE CNODEL - Pulls out quantities for the current element from the global nodal array and restores them in the element work space. Coordinate transformations necessary for beam and shell elements are performed in this subprogram.

SUBROUTINE DERIV - Sets up the displacement-strain matrix for the current element by calling the element library subroutines. Those are:

SUBROUTINE BPSTRS for plane stress elements, types 3 and 101.

SUBROUTINE BPSTRN for plane strain elements, types 11 and 102.

SUBROUTINE BSOLID for three-dimensional solid element, type 7.

SUBROUTINE BSHELL for three-dimensional shell element, type 75.

SUBROUTINE BAXSYM for axisymmetric solid-of-revolution elements, types 10 and 103.

SUBROUTINE BTBEAM for linear Timoshenko beam element, type 98.

SUBROUTINE BASPST for the assumed stress plane stress element, type 151.

SUBROUTINE BASPSN for the assumed stress plane strain element, type 152.

SUBROUTINE BASSOL for the assumed stress three-dimensional solid element, type 154.

SUBROUTINE UDERIV - A slot for a user coded element **B** matrix routine.

The following subprograms are used to calculate terms appearing in the finite element equations:

SUBROUTINE LMPMAS - Calculates nodal weight factors for the strain projection.

SUBROUTINE STIFF - Performs matrix triple products to assemble the element stiffness matrix and the element load vector associated with the initial strain terms.

SUBROUTINE STRAIN - Calculates element strains at specified sampling points and projects to nodes.

SUBROUTINE CNSMAS - Assembles the consistent mass matrix for modal and transient analysis.

SUBROUTINE INITST - Generates initial stress terms for quasi-static, buckling and modal analysis of prestressed structures.

SUBROUTINE CENMAS - Evaluates the centrifugal mass terms for rotating structures at speed.

SUBROUTINE RESID - Calculates the element residual vector for the global element.

SUBROUTINE SUBFEM - Performs the subelement solution and calculates the element residual vector for the subelement mesh.

SUBROUTINE RELDFG - Calculates the relative deformation gradient at the element sampling point and projects to a node.

SUBROUTINE RESDYN - Calculates the contribution of mass and damping terms in the element residual vector when the transient dynamics option is used.

Material Library

A system of subroutines is included in the MHOST code which covers a wide range of material models and initial strain assumptions:

SUBROUTINE SIMPLE - Integrates the stress over the increment assuming the elastic-plastic response of the material is represented by a total nonlinear elastic secant modulus. Also generates the material modulus matrix.

SUBROUTINE PLASTS - Integrates the stress over the increment and calculates the plastic strain by using the radial return algorithm.

SUBROUTINE PLASTD - Calculates a consistent elastic-plastic modulus if the incremental equivalent plastic strain is positive.

SUBROUTINE WALKEQ - Integrates the Walker unified creep plasticity constitutive equation and also generates a material modulus based on the temperature dependent elasticity assumption.

SUBROUTINE LELAST - Calculates the stress for the constant material modulus given as data.

SUBROUTINE THRSTN - Calculates the thermal strain.

SUBROUTINE CRPSTN - Calculates the creep strain.

4.3 USER INTERFACE

A large number of options are made available in the MHOST code. A user selects options by specifying certain keywords in the parameter data section of the input data file. Some of the infrequently used features available in the previous versions are deleted for the sake of clarity. Table 2 summarizes the analysis capability of MHOST Version 4.2.

Table 2 MHOST Analysis Capability

Element Definition Options	Beam	Plane Stress	Plane Strain	Axisymmetric Solid	Three-Dimensional Solid	Three-Dimensional Shell
Linear Isotropic Elasticity	x	x	x	x	x	x
Anisotropic*1 Elasticity		x	x	x	x	
Composite*1 Laminate						x
Simplified Plasticity		x	x	x	x	x
Elasto-*3 Plasticity		x	x	x	x	x
Unified Creep-Plasticity		x	x	x	x	x
Thermal*2 Strain		x	x	x	x	x
Creep*2 Strain		x	x	x	x	x
Large Displacement	x	x	x	x	x	x
Finite Strain		x	x	x	x	

Notes:

*1 Applicable only to linear elasticity.

*2 Not applicable to the unified creep-plasticity model in which the quantities are the integrated part of the model.

*3 Anisotropic yield surface can be defined for a continuum element.

Table 2 MHOST Analysis Capability (continued)

Analysis Module Option	Beam	Plane Stress	Plane Strain	Axisymmetric Solid	Three-Dimensional Solid	Three-Dimensional Shell
Quasi-static Analysis	x	x	x	x	x	x
Buckling Analysis	x	x	x	x	x	x
Modal Analysis	x	x	x	x	x	x
Transient Dynamics	x	x	x	x	x	x

In the model data section of the input data file, certain nonstandard features are made available. This subsection summarizes program features available in Version 4.2 of the MHOST code by the keywords. For full details, see the MHOST User's Manual.

*ANISOTROPY

The anisotropic material property option is flagged by this parameter. The orientation vector for the material axes must be added in the model data section. The material properties along the material axes must be given by either the *DMATRIX option (for continuum elements, type 3, 7, 10 and 11) or the *LAMINATE option (for shell element type 75). The anisotropic plastic response of a material is described by the user subroutine ANPLAS as documented in the MHOST User's Manual.

*BFGS

The inverse BFGS update procedure is invoked by flagging this option parameter with the default iterative algorithm being the straightforward Newton-Raphson scheme.

*BOUNDARY

The nodal displacement constraints are imposed by virtue of penalization when the frontal solution subsystem is invoked.

*BUCKLE

The initial stress matrix is generated and the eigenvalue extraction is performed to obtain buckling modes. This option can be invoked at an arbitrary step of the incremental nonlinear solution process so as to detect the change in the buckling load due to the inelastic response of the structure.

*COMPOSITE

This parameter data line invokes the composite laminate analysis option for shell element type 75. Added to the MHOST code upon request from the Contract Monitor at NASA-Lewis Research Center. This option resets the element parameters. The number of integration layers is reduced to 1 and all the components of stress resultant are used as nodal variables. In the model data section, the user has to supply all the components of the stress-strain matrix by invoking the laminate option.

*CONJUGATE-GRADIENT

The conjugate-gradient method is invoked by adding this parameter. The line search option is automatically turned on. Note that this option cannot be used with other iterative algorithms such as the BFGS or secant-Newton methods.

*CONSTITUTIVE

Three constitutive approaches are available for describing material behavior, including the secant elasticity procedure (simplified plasticity) in which the material tangent is generated for Newton-Raphson type iterative algorithms, the von Mises plasticity procedure with the associated flow rule treated by the radial return algorithm, and the Walker nonlinear viscoplastic model in which an initial stress iteration using elastic stiffness is utilized. For experimental purposes, the linear elasticity option can be flagged, with the default option being the conventional plasticity model.

*CREEP

The creep effect is taken into account via the time history being integrated in an explicit manner under control of an optional self adaptive time-step size algorithm.

*DISPLACEMENTMETHOD

This option invokes the conventional displacement model in which the residual loads are evaluated directly at integration points. For linear elastic stress analyses, no iteration would take place when this parameter card is flagged. In inelastic analyses, the material tangent is interpolated and multiplied by integration point strains directly at each quadrature point. This option cannot be used for the creep-plasticity model which does not generate correct material tangent information at integration points.

*DISTRIBUTELOAD

The body force and surface traction loadings are referred to as the distributed loads in the MHOST program. The body force option includes gravity acceleration definable in any direction, as well as centrifugal loading with the centerline and angular velocity being user-specified.

*DUPLICATENODE

The nodal points for stress recovery can be disconnected by defining two nodal points at the same geometrical location and connecting them by this option which assumes the compatibility of displacement at these points. This option is used to define generic modeling regions and their interconnections.

*DYNAMIC

The generalized Newmark solution algorithm is entered by using this parameter card. A primitive version of the adaptive time-stepping algorithm is incorporated if requested by the user.

*ELEMENTS

The elements available in this version of the code are summarized in Table 3. Core allocation is performed for both nodal- and element-quantities based on the maximum storage space requirements among the types of element specified in this option. All the element types must be specified here, including those only associated with the subelement regions.

*EMBED

The subelement iteration technology is flagged by this option to signal the code to allocate working storage for subelement data in a hierarchical manner.

The actual subelement mesh definition and the nodal- and element-data storage allocation take place when the individual subelement is defined.

*FINITE_STRAIN

This keyword invokes the finite-strain option at a specified load/time increment.

*FOLLOWER_FORCE

The loading data is assumed as the follower force when this keyword is included in the parameter data section.

*FORCES

Concentrated nodal forces are defined and stored in an incremental manner. The core allocation takes place only when this option is invoked.

*FRONTALSOLUTION

The frontal solution option for quasi-static analysis is available in this version of the code and utilizes out-of-core storage devices, thus increasing the capacity of the program significantly.

*HARDENING_SLOPE

The maximum number of break points for a piecewise linear approximation of uniaxial elastic-plastic behavior is specified with this parameter keyword.

*LARGE_DISPLACEMENT

This keyword invokes the large displacement option at the specified load/time increment.

*LINE-SEARCH

The line search option requires positive action by the user to be turned on. This algorithm is usable in conjunction with all iteration algorithms available in the MHOST program. When the conjugate-gradient iteration is used, the program automatically turns on the line search option.

*LOUBIGNAC

Parameters for numerical quadrature used in mixed iterative processes are definable in a very precise way. To construct the stiffness matrix the full, selective, or selective with filtering scheme can be chosen. For the residual vector integration, full or reduced integration can be chosen. The strain integration can be performed by using either uniformly reduced integration, trapezoidal integration with a reduced shear strain approximation, or trapezoidal integration with a filtering option.

*MODAL

Free vibration modes are extracted by invoking this option for linear elastic structures only. The subspace iteration technique is utilized together with the power shift option.

*NODES

All the variables are defined and reported at nodal points. In the incremental processes, the deformation and stress history are stored only at the nodal points. Note that this architecture economizes storage substantially as compared to the fully integrated finite element displacement methods.

*NOECHO

This option suppresses the echo print of the model data.

*OPTIMIZE

Bandwidth optimization based on the Cuthill-McGee algorithm is available in the MHOST code, whereas no optimization for the frontal solver is available.

*PERIODICLOADING

For transient analyses, nodal displacements and concentrated forces can be given as sinusoidal functions via this option; this reduces the effort needed to prescribe the load history for a class of simple test problems.

*POST

The post-processing file, which contains all the information supplied to and produced by the code, is generated on the file connected to FORTRAN unit number 19. This file is formatted and can easily be manipulated by commercially available post-processing packages with minor modifications. A version of MENTAT supports the MHOST post-processing file. The header record of the file is designed to be compatible with the MARC post file, details of which are published and processed by many finite element graphics packages.

*PRINTSETS

Report generation is carried out on a nodal point basis, with the element integration point option supported by interpolation processes using appropriate shape functions.

*REPORT

The frequency of the line printer report generation is now controlled by this option with the default being to print at every increment.

*RESTART

This parameter card invokes the program to read the restart tape and to set up the system to resume the analysis from the point where the tape is written.

*SCHEME

Parameters for defining characteristics of the time integration operator can be specified by the user. The default is the average acceleration algorithm commonly used in nonlinear dynamic finite element analyses.

*SECANT-NEWTON

This parameter activates the secant-Newton implementation of the Davidon rank-one quasi-Newton algorithm. The core-storage requirements of this procedure are significantly less than for the BFGS update and the execution is relatively fast. This parameter is recommended for inelastic analyses of solid-continua.

*STIFFENING

This keyword is used to invoke initial stress terms for quasi-static, transient dynamic and modal analyses.

*STRESS

As an option, the boundary condition for stress can be specified by the user, although no mathematical justification is yet available for this type of boundary loading. Any stress component can be prescribed at any nodal point. Simple numerical tests have shown that inconsistent imposition of boundary stress values indeed lead to rapid divergence in the iterative process.

*TANGENT

In the context of modified Newton iterations, the tangent stiffness matrix for subsequent iterations is user-definable. When this option is invoked, the default is the first tangent matrix used during the current increment, not the elastic stiffness matrix. This type of implementation is referred to as the K_{T1} method of modified Newton iteration. In the BFGS process, the same approach is used and no options are made available. In the modified Newton iteration, the tangent array is fixed after a specified number of updates.

*TEMPERATURE

Nodal temperatures are read as input and used to generate thermal strains. These temperatures are used also during the evaluation of creep strains and the integration of the coupled creep plasticity model (Walker's model).

*THERMAL

Temperature dependent material properties are evaluated when this option is invoked, and an appropriate user subroutine has to be provided to the system prior to execution. This operation is not necessary for the creep plasticity model in which the temperature dependency is readily incorporated.

*TRANSFORMATIONS

Coordinate transformations at nodal points are specified by this option in which the angle of rotation is provided by the user so that the code can generate necessary transformation matrices. The post-processing file does not support the coordinate transformations.

*TYING

Multiple degree-of-freedom constraint equations are specified by the user through this option. Under certain circumstances, this option is slightly more flexible than the duplicate node option; for instance, the user can disconnect three elements at a point. Note that the constraint equations are generated only for displacement degrees-of-freedom, which are calculated only in an implicit manner.

The following parameters are used to signal to the MHOST program the presence of specific user subroutines:

*UBOUN
*UCOEF
*UDERIV
*UFORCE
*UHOOK
*UPRESS
*UTEMP
*UTHERM
*WKSLP

As summarized above, the analysis capabilities included in the MHOST code cover most requirements for calculating inelastic deformations of turbine engine hot section components. The MHOST code has evolved into a General Purpose Structural Analysis package with strong emphasis on nonlinear material behavior usable for a wide range of problems. The free format data input routines and report generation packages have been improved in the Task II program development effort so as to create a comfortable environment for code users.

Table 3 summarizes the elements currently available in the MHOST Version 4.2 code and lists parameters internally used to define element characteristics. Further detail is available in the MHOST User's Manual.

Table 3 Element Parameters

	Beam	P.Stress	P.Strain	Axsym.	Brick	Shell
ITYPE	9	3/101/151	11/102/152	10/103/153	7/154	75
NELCRD	3	2	2	2	3	3
NELNFR	3	2	2	2	3	6
NELNOD	2	4/9/4	4/9/4	4/9/4	8	4
NELSTR	1	3	4	4	6	8
NELCHR	3	5	5	5	5	5
NELINT	2	4/9/4	4/9/4	4/9/4	8	4
NELLV	3	3	3	3	3	4
NELLAY	0	1	1	1	1	5
NDI	1	2	3	3	3	2
NKHEAR	0	1	1	1	3	1
JLAW	1	2	3	4	5	6

NELCRD Number of coordinate point data values per node.

NELNFR Number of degrees-of-freedom per node.

NELNOD Number of nodes per element.

NELSTR Number of stress and strain components per node.

NELCHR Number of material property data values for the element.

NELINT Number of 'full' integration points per element.

NELLV Number of distributed load types per element.

NELLAY Number of layers of integration through the thickness of the shell element.

NDI Number of direct stress components.

NSHEAR Number of shear stress components.

JLAW Type of the constitutive equation.

4.4 VALIDATION

4.4.1 Performance Improvement by the Profile Solver

Table 4 summarizes computing time and memory requirement reductions after implementation of the profile solver solution package into the MHOST code. The performance figures are applicable for the MARC Corp. PRIME 9955 computer using a Primos FORTRAN 77 compiler with the full optimization option turned on. The number of words appearing in the table apply to situations involving single precision (32 bits) words in the blank common work space. For 64 bits/word machines such as CRAY, the memory requirement in terms of number of words will be considerably smaller. Even for a system of uniformly banded equations such as occurs with the composite laminate fan blade shown in Figure 4, a substantial reduction in computing time and some improvement in core-storage requirements are obtained with the profile solver package.

For large problems such as the turbine blade model with platform as shown in Figure 2, the speed gain and reduction in memory needed make an in-core solution possible on a small computer.

In a buckling analysis of the cylinder whose mesh is shown in Figure 3, the reduction in solution time is an order of magnitude more significant than the saving in storage requirements.

Note that the tying option for the profile solver is implemented in a global manner. The algebraic constraint equations are embedded in the profile-form stiffness matrix after all the element matrices are assembled. On the other hand, the coordinate transformation option for the nodal degrees-of-freedom is handled on an element-by-element basis. Immediately after an element matrix is assembled, the entries subjected to coordinate transformations are manipulated before substituting into the global array.

Table 4 Performance Tests for the Profile Solver Solution Package in the MHOST Code

Problem 1 SSME HPFTP Blade Model with 1025 Solid Elements (Type 7) and 1575 Nodes (Mesh Shown in Figure 2)

	Profile Solver	Band Solver
Working Space Required	3,483,811	4,459,647
Solution Time (seconds)	1466.594	NA*

*Too large to be able to run on PRIME 9955 at MARC.

Problem 2 Buckling Analysis of a Cylinder with 160 Shell Elements (Type 75) and 176 Nodes (Mesh Shown in Figure 3)

	Profile Solver	Band Solver
Working Space		
- Static	498,873	596,703
- Eigenvalue	1,044,773	1,340,375
Solution Time (seconds)		
- Static	62.057	171.430
- Eigenvalue	66.788	187.551

Problem 3 Modal Analysis of Composite Laminate Fan Blade with 240 Shell Elements (Type 75) and 279 Nodes (Mesh Shown in Figure 4)

	Profile Solver	Band Solver
Working Space	824,341	1,054,259
Solution Time (seconds)	24.794	93.764

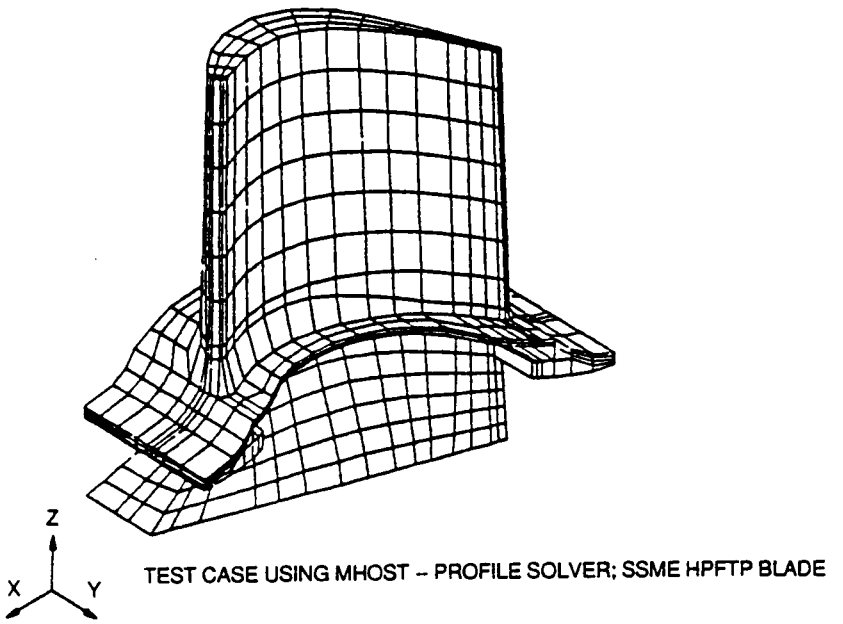

Figure 2 Finite Element Mesh for Problem 1 (Turbine Blade Model with Platform)

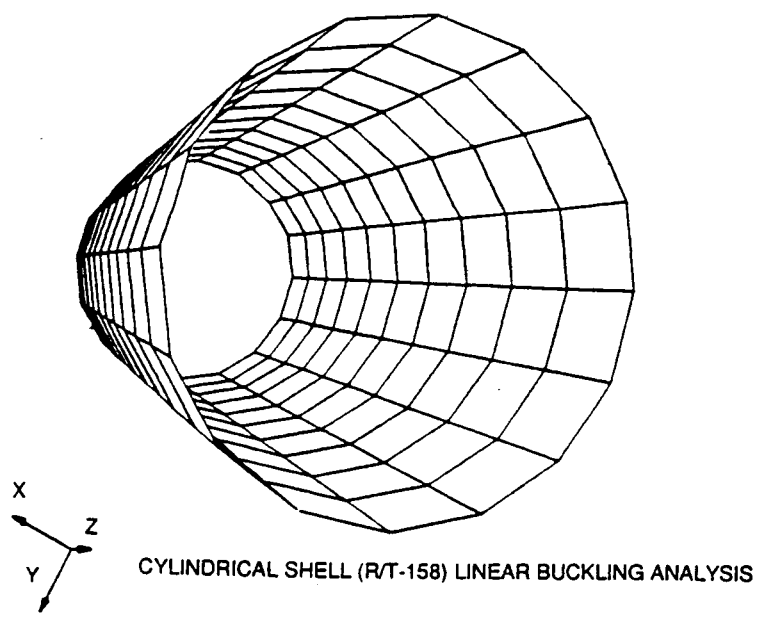

Figure 3 Finite Element Mesh for Problem 2 (Buckling Analysis of a Cylinder)

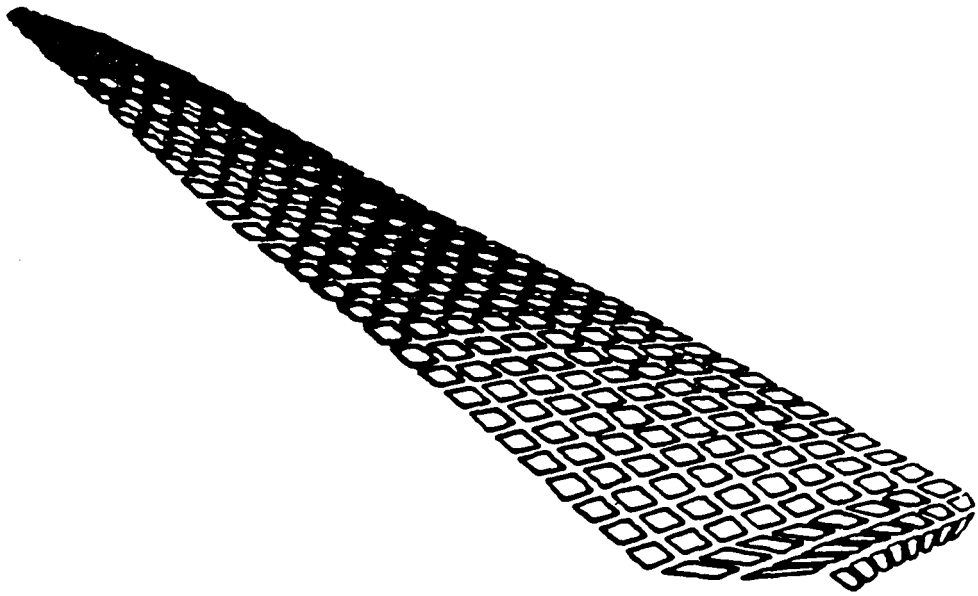

Figure 4 Finite Element Mesh for Problem 3 (Composite Laminate Fan Blade)

4.4.2 Vibration Analysis of a Rotating Beam

The stress stiffening and centrifugal mass options were validated by analyzing a cantilever beam rotating at a given angular velocity, with the geometry and loading conditions illustrated in Figure 5. Two finite element models were constructed on MHOST, one using the shell element (type 75) and one using the three-dimensional solid element (type 7). A reference solution was also established: a solution on NASTRAN using its shell element (QUAD4) was compared with a solution produced by MARC via its shell element (type 75). Both commercial codes produce almost identical vibration frequencies which establish the reference solution. As the values in Table 5 indicate, both MHOST solutions are almost identical to the reference solution. This also indicates that the selectivity integrated linear solid element is capable of accurately representing bending mode response.

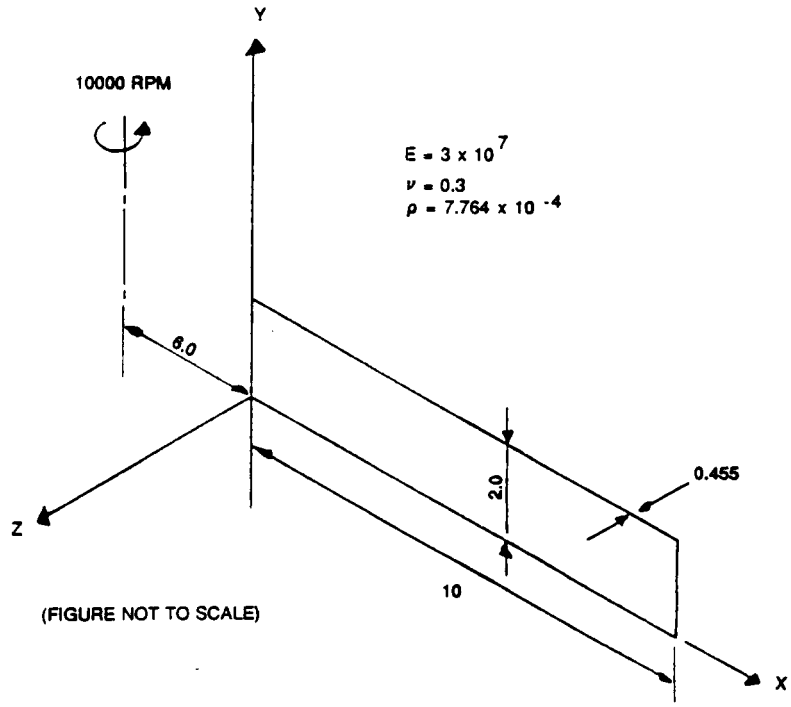

Figure 5 Validation Model for Centrifugal Stiffening

Table 5 Vibration Frequency-Cantilever Beam Under Centrifugal Loading (Column A: Without Stiffening; Column B: With Stiffening and Centrifugal Mass)

Mode	NASTRAN Shell Element**		MHOST Shell Element		MHOST Solid Element	
	A	B	A	B	A	B
1*	145.4	227.6	145.4	228.7	145.8	229.9
2	618.9	662.3	628.6	668.2	595.8	669.3
3	894.8	1042.8	924.5	1077.0	929.9	1089.0
4	1115.0	1199.0	1316.7	1375.8	1205.1	1229.2

* MARC shell element type 75 gives 146.2 Hz without centrifugal stiffening and 228.3 Hz with the stiffening and centrifugal mass effects included.

** Element type QUAD4.

4.4.3 Large Displacement Analysis

A plane stress test problem involving stretching an elastic-plastic plate is analyzed using the large displacement analysis capabilities of the MHOST code. Listing 1 shows the input data used for the calculations. The original finite element mesh, as well as a deformed configuration, are plotted in Figure 6. The solution obtained is smooth without any indication of numerical instabilities. Equivalent plastic strain and Mises equivalent stress plots are shown in Figures 7 and 8 respectively.

Listing 1 Input Data for a Large Displacement Analysis by Plane Stress Elements

```
ELASTIC PLASTIC ALUMINUM PLATE-8X8 PLANE STRESS-L 313
*POST
*NODES 81
*ELEMENTS 64
   3
*CONSTITUTIVE 2
*HARD 2
*BOUNDARY 40
*LARGE_DISPLACEMENT
*FINITE_STRAIN
*STIFFENING
*LOUBIGNAC 3 1 3
*END
*WORKHARD 2
   45000.0  0.0000  0.0000
  850000.0  10.000  0.0000
*ITERATIONS
   20   0.050
*COORDINATES
    1    0.0000    0.0000    0.0000    0.05000
    2    0.0000    1.0000    0.0000
    3    0.0000    2.0000    0.0000
    4    0.0000    3.0000    0.0000
    5    0.0000    4.0000    0.0000
```

6	0.0000	5.0000	0.0000
7	0.0000	6.0000	0.0000
8	0.0000	7.0000	0.0000
9	0.0000	8.0000	0.0000
10	1.0000	0.0000	0.0000
11	1.0000	1.0000	0.0000
12	1.0000	2.0000	0.0000
13	1.0000	3.0000	0.0000
14	1.0000	4.0000	0.0000
15	1.0000	5.0000	0.0000
16	1.0000	6.0000	0.0000
17	1.0000	7.0000	0.0000
18	1.0000	8.0000	0.0000
19	2.0000	0.0000	0.0000
20	2.0000	1.0000	0.0000
21	2.0000	2.0000	0.0000
22	2.0000	3.0000	0.0000
23	2.0000	4.0000	0.0000
24	2.0000	5.0000	0.0000
25	2.0000	6.0000	0.0000
26	2.0000	7.0000	0.0000
27	2.0000	8.0000	0.0000
28	3.0000	0.0000	0.0000
29	3.0000	1.0000	0.0000
30	3.0000	2.0000	0.0000
31	3.0000	3.0000	0.0000
32	3.0000	4.0000	0.0000
33	3.0000	5.0000	0.0000
34	3.0000	6.0000	0.0000
35	3.0000	7.0000	0.0000
36	3.0000	8.0000	0.0000
37	4.0000	0.0000	0.0000
38	4.0000	1.0000	0.0000
39	4.0000	2.0000	0.0000
40	4.0000	3.0000	0.0000

41	4.0000	4.0000	0.0000
42	4.0000	5.0000	0.0000
43	4.0000	6.0000	0.0000
44	4.0000	7.0000	0.0000
45	4.0000	8.0000	0.0000
46	5.0000	0.0000	0.0000
47	5.0000	1.0000	0.0000
48	5.0000	2.0000	0.0000
49	5.0000	3.0000	0.0000
50	5.0000	4.0000	0.0000
51	5.0000	5.0000	0.0000
52	5.0000	6.0000	0.0000
53	5.0000	7.0000	0.0000
54	5.0000	8.0000	0.0000
55	6.0000	0.0000	0.0000
56	6.0000	1.0000	0.0000
57	6.0000	2.0000	0.0000
58	6.0000	3.0000	0.0000
59	6.0000	4.0000	0.0000
60	6.0000	5.0000	0.0000
61	6.0000	6.0000	0.0000
62	6.0000	7.0000	0.0000
63	6.0000	8.0000	0.0000
64	7.0000	0.0000	0.0000
65	7.0000	1.0000	0.0000
66	7.0000	2.0000	0.0000
67	7.0000	3.0000	0.0000
68	7.0000	4.0000	0.0000
69	7.0000	5.0000	0.0000
70	7.0000	6.0000	0.0000

```
   71     7.0000     7.0000     0.0000
   72     7.0000     8.0000     0.0000
   73     8.0000     0.0000     0.0000
   74     8.0000     1.0000     0.0000
   75     8.0000     2.0000     0.0000
   76     8.0000     3.0000     0.0000
   77     8.0000     4.0000     0.0000
   78     8.0000     5.0000     0.0000
   79     8.0000     6.0000     0.0000
   80     8.0000     7.0000     0.0000
   81     8.0000     8.0000     0.0000
*ELEMENTS 3
    1    1    10    11    2
    2    2    11    12    3
    3    3    12    13    4
    4    4    13    14    5
    5    5    14    15    6
    6    6    15    16    7
    7    7    16    17    8
    8    8    17    18    9
    9   10    19    20   11
   10   11    20    21   12
   11   12    21    22   13
   12   13    22    23   14
   13   14    23    24   15
   14   15    24    25   16
   15   16    25    26   17
   16   17    26    27   18
   17   19    28    29   20
   18   20    29    30   21
   19   21    30    31   22
   20   22    31    32   23
```

21	23	32	33	24
22	24	33	34	25
23	25	34	35	26
24	26	35	36	27
25	28	37	38	29
26	29	38	39	30
27	30	39	40	31
28	31	40	41	32
29	32	41	42	33
30	33	42	43	34
31	34	43	44	35
32	35	44	45	36
33	37	46	47	38
34	38	47	48	39
35	39	48	49	40
36	40	49	50	41
37	41	50	51	42
38	42	51	52	43
39	43	52	53	44
40	44	53	54	45
41	46	55	56	47
42	47	56	57	48
43	48	57	58	49
44	49	58	59	50
45	50	59	60	51
46	51	60	61	52
47	52	61	62	53
48	53	62	63	54
49	55	64	65	56
50	56	65	66	57

```
   51   57   66   67   58
   52   58   67   68   59
   53   59   68   69   60
   54   60   69   70   61
   55   61   70   71   62
   56   62   71   72   63
   57   64   73   74   65
   58   65   74   75   66
   59   66   75   76   67
   60   67   76   77   68
   61   68   77   78   69
   62   69   78   79   70
   63   70   79   80   71
   64   71   80   81   72
*BOUNDARY
  1  1
  1  2
  2  1
  3  1
  4  1
  5  1
  6  1
  7  1
  8  1
  9  1
 10  2
 19  2
 28  2
 37  2
 46  2
 55  2
 64  2
 73  1   0.8000
 73  2
```

```
 74  1    0.8000
 74  2
 75  1    0.8000
 75  2
 76  1    0.8000
 76  2
 77  1    0.8000
 77  2
 78  1    0.8000
 78  2
 79  1    0.8000
 79  2
 80  1    0.8000
 80  2
 81  1    0.8000
 81  2
*PROPERTIES  3
C     STANDARD ALUMINUM MATERIAL
  1  81  0.05  10.0E6  0.330
*PRINTOPTION
INCREMENTALDISPLACEMENT NODE
TOTALDISPLACEMENT       NODE
REACTION                NODE
PLASTIC                 NODE
STRESS                  NODE
STRAIN                  NODE
FORCE                   NODE
*END
*AUTOINCREMENT
      9
*END
*STOP
```

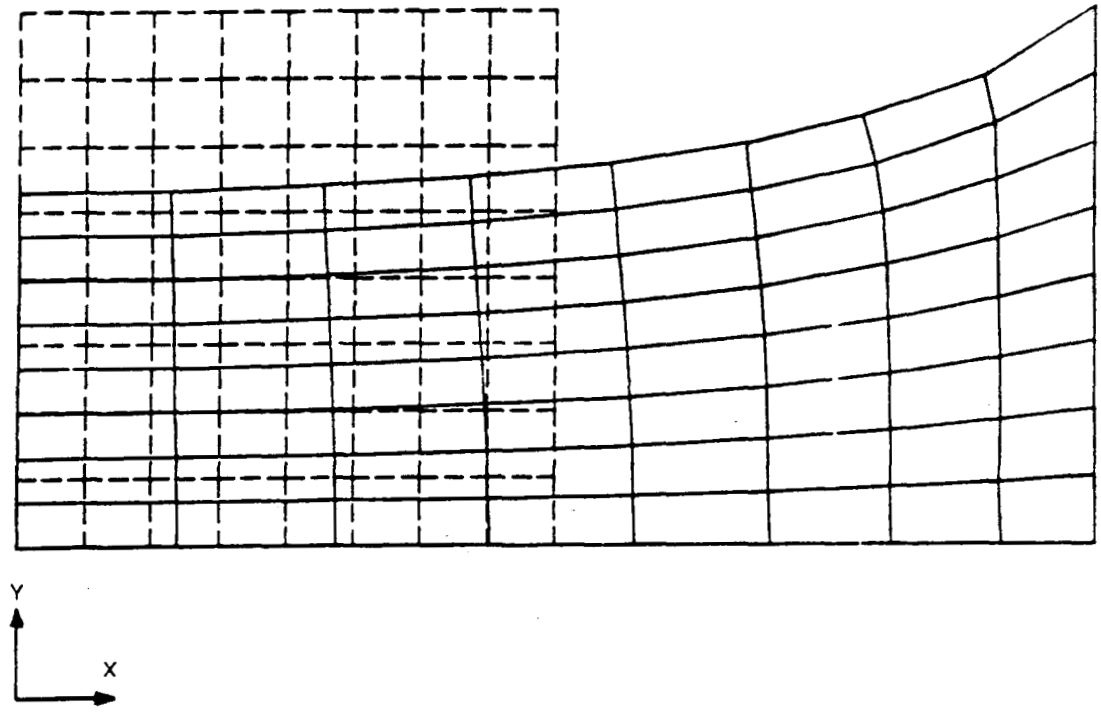

Figure 6 Elastic-Plastic Membrane; Deformed Shape

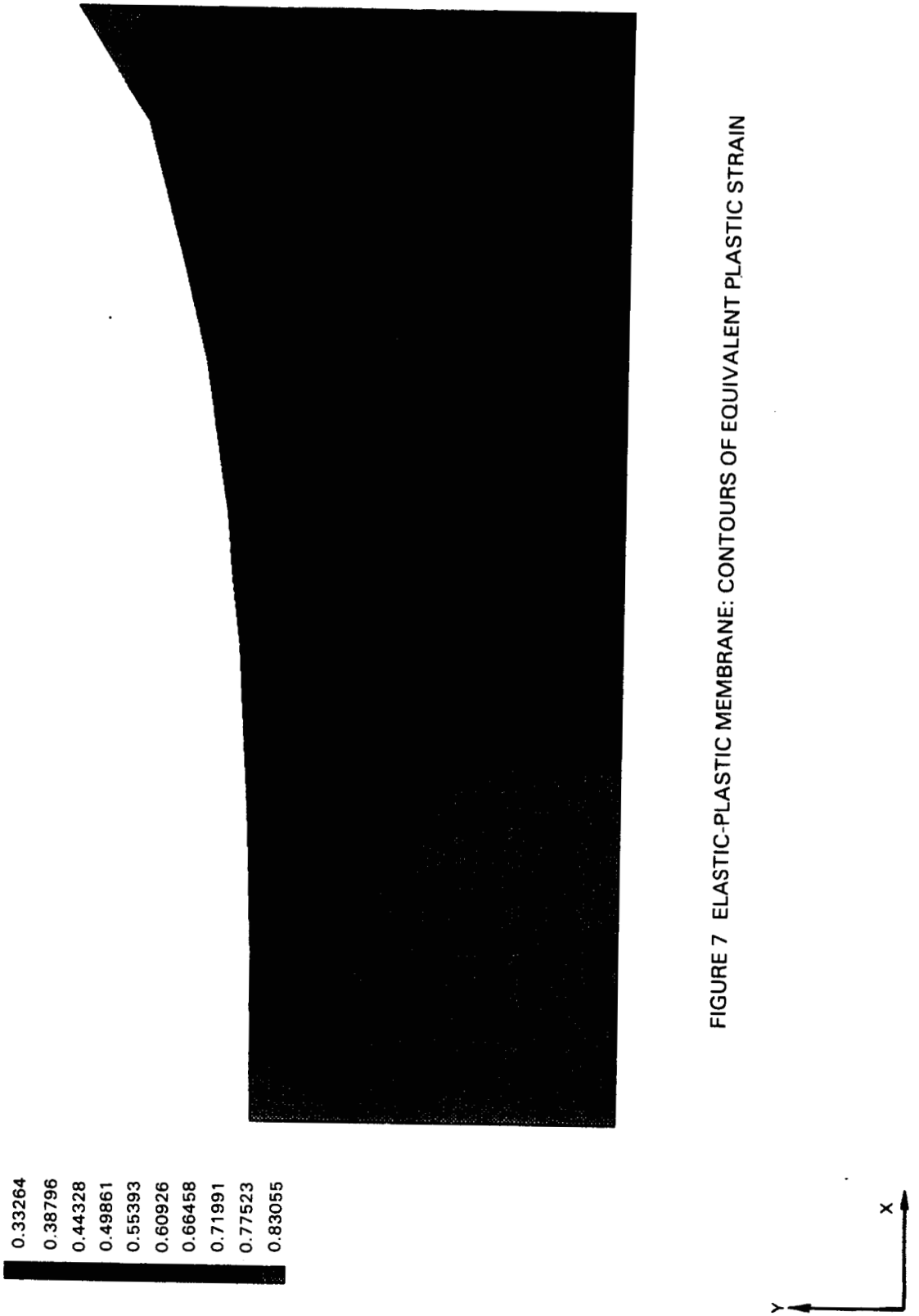

FIGURE 7 ELASTIC-PLASTIC MEMBRANE: CONTOURS OF EQUIVALENT PLASTIC STRAIN

ORIGINAL PAGE
COLOR PHOTOGRAPH

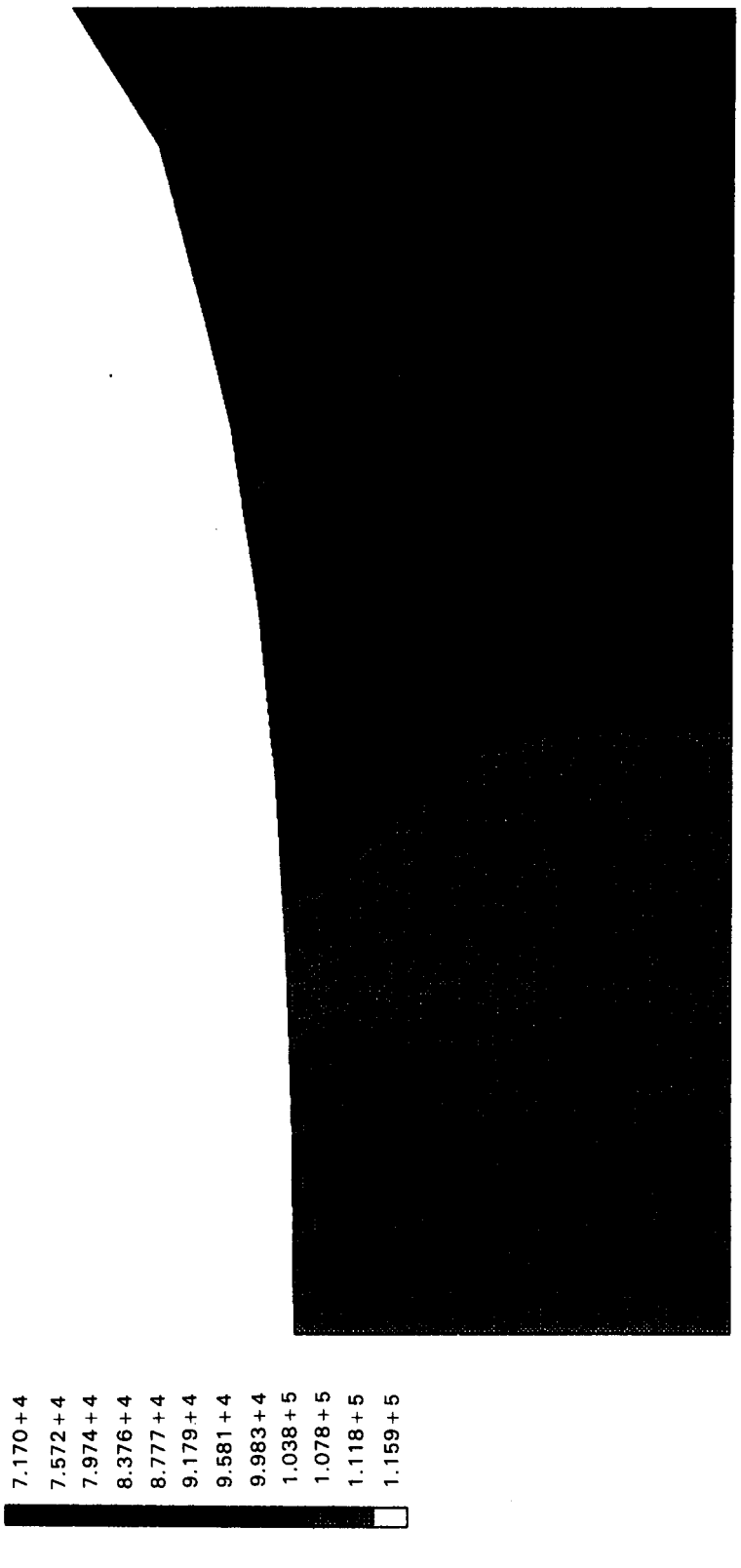

FIGURE 8 ELASTIC-PLASTIC MEMBRANE: CONTOURS OF MISES STRESS

A disc upsetting problem involving both large displacement and large strain behavior is used as a second example. This is a standard problem solved repeatedly by MARC, and the reference solution is readily available. As the initial mesh and deformed configuration plots (Figure 9) indicate, a large amplitude hourglassing is observed. This is due to the nearly incompressible response of the material and the same phenomenon with less significant amplitude is observable in a standard displacement solution. Further investigation on stabilization of the displacement field is necessary to filter out this spurious mode. However, the stress field obtained with the present capability is stable and quantitatively agrees well with the solution obtained by MARC via the conventional displacement method (Figure 10).

For comparison, the same disc upsetting problem is studied using the three-dimensional solid element (Figure 11). As indicated in the stress contour plot (Figure 11) at an early stage of the deformation process, the model is capable of reproducing an axisymmetric stress field quantitatively similar to that generated using the axisymmetric element.

As an example of MHOST's large displacement analysis capability with shell elements, a one-quarter model of a clamped square plate under uniform pressure loading is studied. The results are plotted in Figure 12, together with solutions of the same problem available in the literature [WAY (1938); KAWAI, YOSHIMURA (1961); HUGHES, LIU (1981); and NAGTEGAAL, SLATER (1981)]. The comparison indicates that the mixed iterative implementation of shell elements results in more flexible behavior compared with the compatible model (Kawai-Yoshimura solution) and with models based on the Reissner-Mindlin theory (Hughes-Liu solution by uniform reduced integration and heterosis elements). Qualitatively, the behavior of the MHOST shell element is similar to the Nagtegaal-Slater solution via the SLICK element derived from the discrete Kirchhoff assumption (MARC element type 72). A visible difference is shown between the solution obtained with 'full' Newton iteration (in which the displacement preconditioner is repeatedly updated) and that obtained via the secant-Newton update with line search. This difference may be due to ill-conditioning of the preconditioner caused by transverse shear constraint terms.

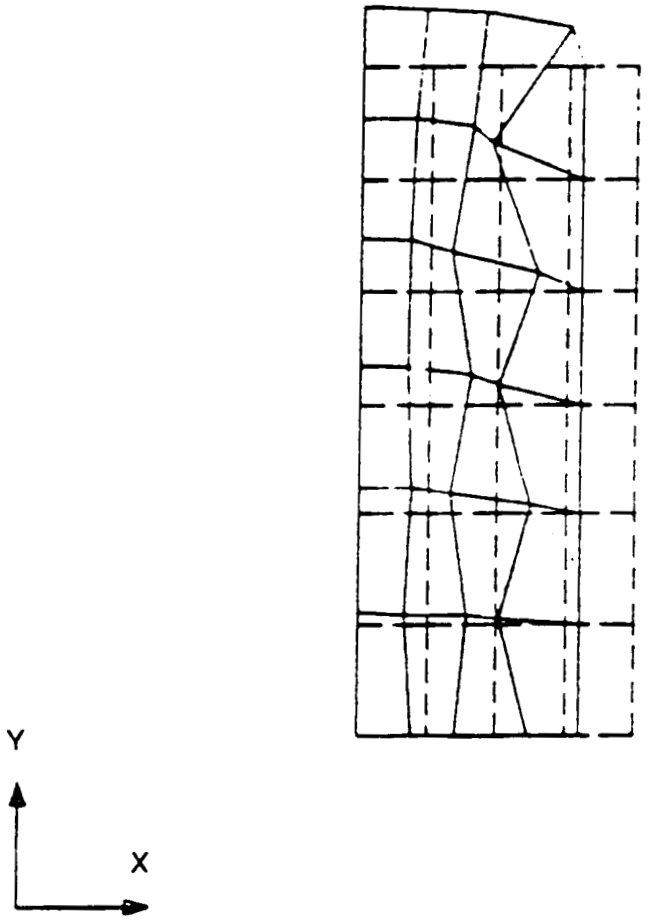

Figure 9 Compression of Solid Axisymmetric Cylinder; Deformed Shape (Hourglassing)

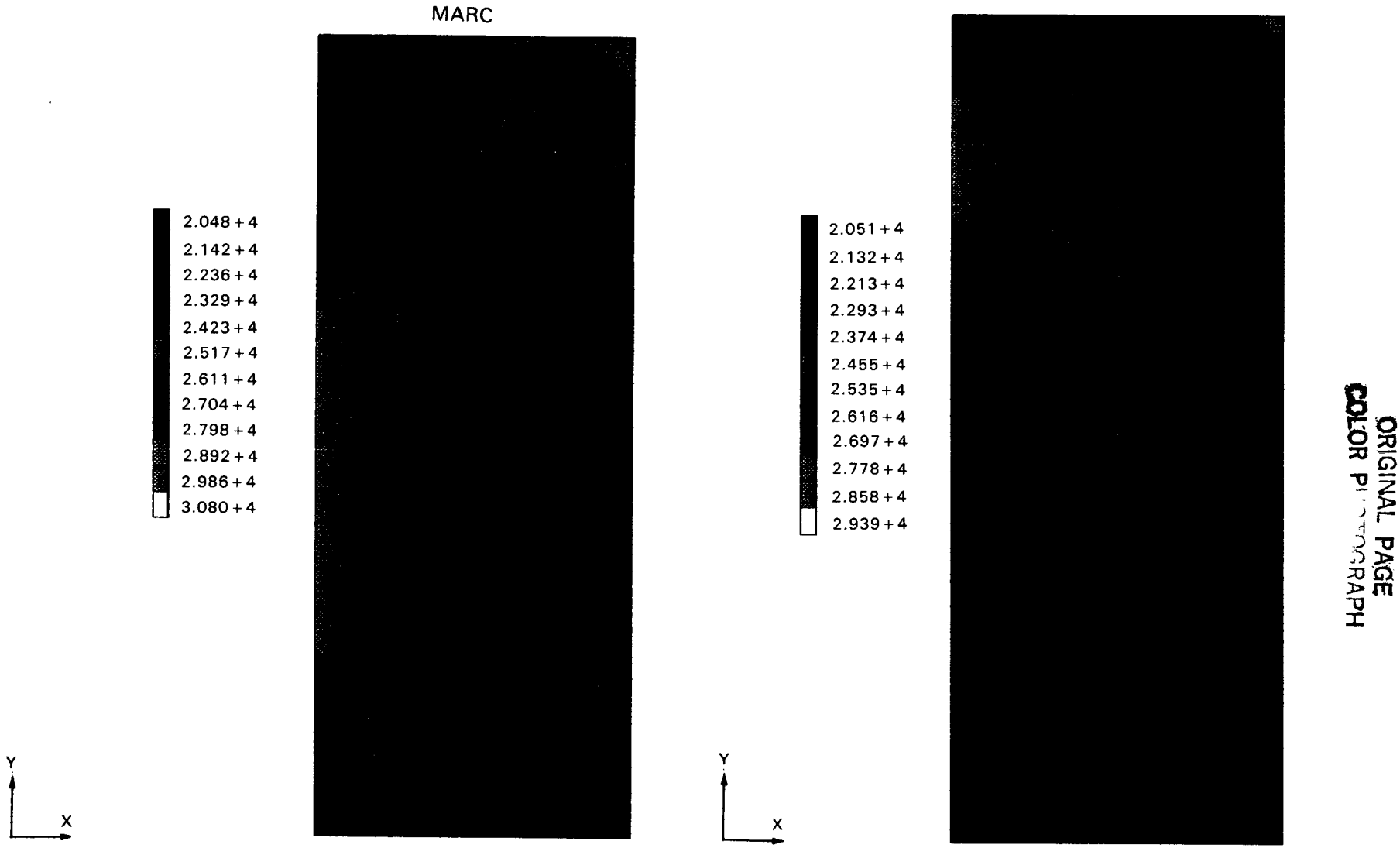

FIGURE 10 AXISYMMETRIC UPSETTING: EQUIVALENT MISES TENSILE STRESS-MHOST VS MARC RESULTS

FIGURE 11 AXISYMMETRIC UPSETTING: EIGHT NODE SOLID MODEL

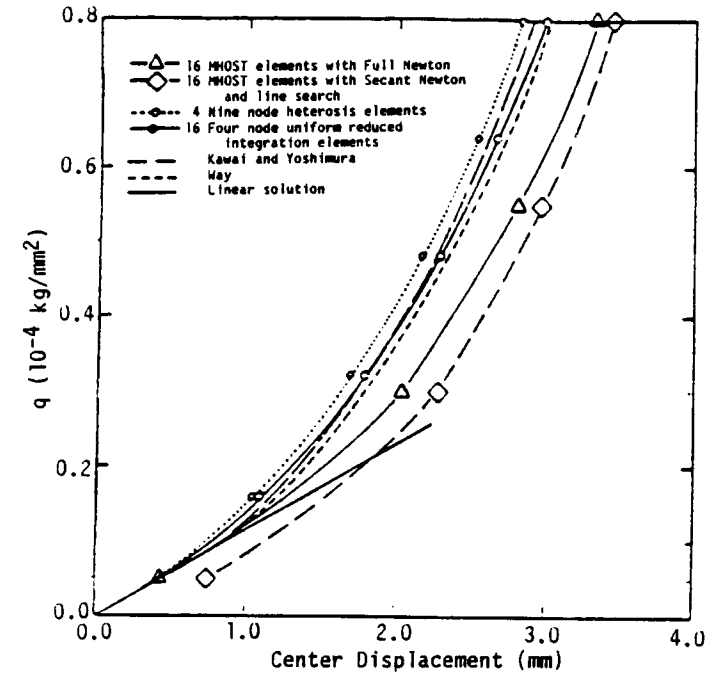

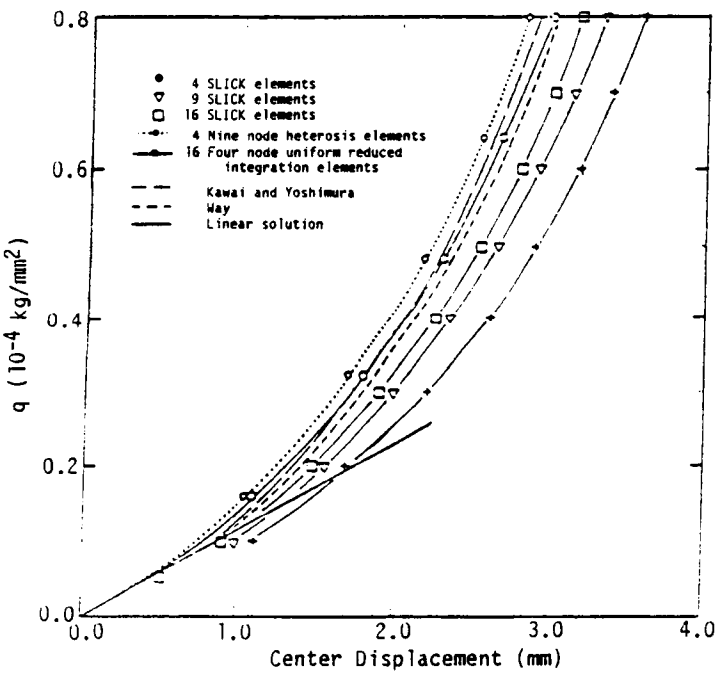

$E = 2 \times 10^4$ kg/mm^2
$\nu = 0.3$
L = 1000 mm
h = 2 mm

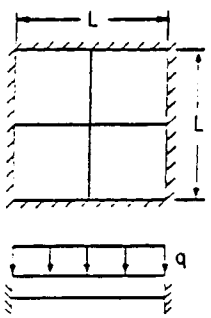

Figure 12 Load Deflection Curves of a Clamped Square Plate Under Uniform Pressure Loading

PRECEDING PAGE BLANK NOT FILMED

4.4.4 Application of the Subelement Method for Inelastic Analysis

A plane stress problem of a square plate with a circular hole is used to demonstrate the inelastic solution capability of the MHOST subelement procedures. The global finite element mesh and the subelement mesh representing a hole embedded in the element at the center of a plate is illustrated in Figure 13. A global finite element model explicitly including the hole in the same way as the subelement grid is shown in Figure 14.

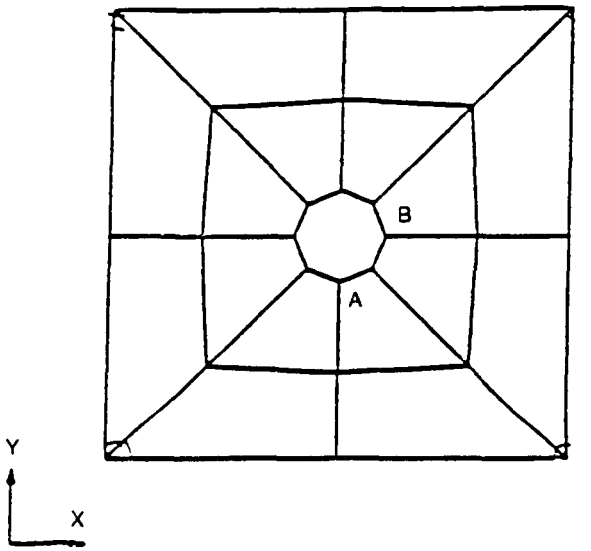

SUBELEMENT MESH FOR AN EMBEDDED HOLE

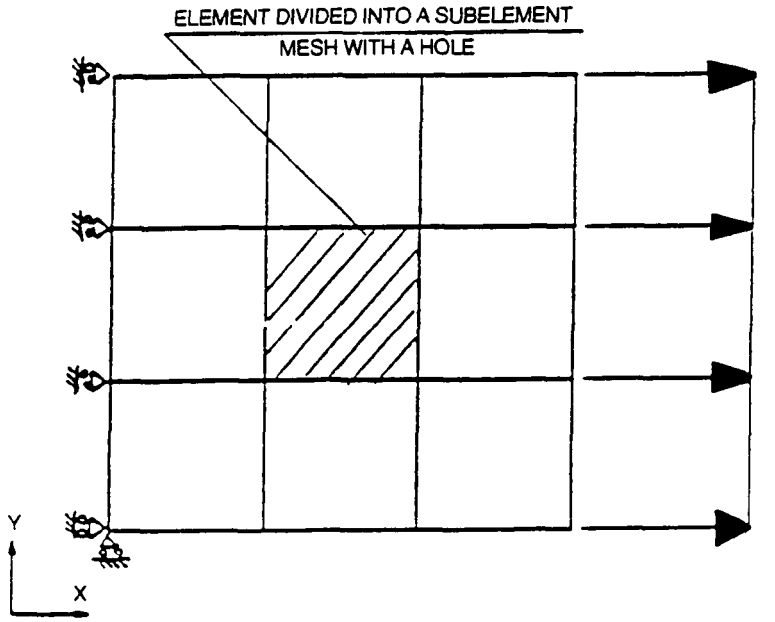

Figure 13 Global and Subelement Meshes for an Embedded Hole

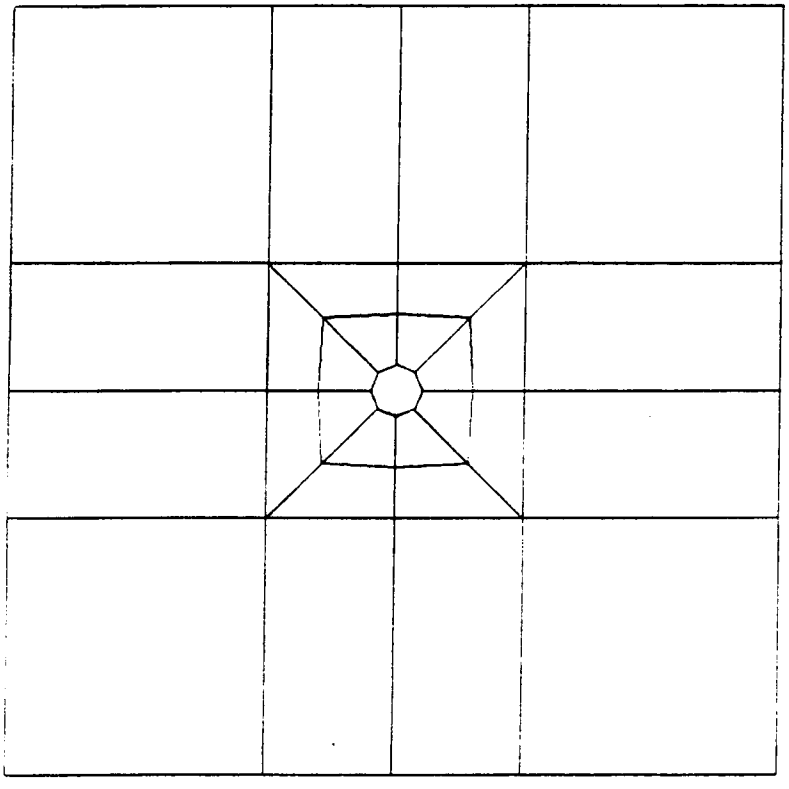

Figure 14 Global Finite Element Mesh

The input data files for both the global element mesh and the subelement mesh models are given in Listings 2 and 3. Note that the amount of data to represent a hole is significantly less for the subelement mesh; this represents a major improvement in user friendliness.

Listing 2 Global Finite Element Model

```
TEST PROBLEM FOR A PLATE WITH A HOLE ( PLANE STRESS )
*POST
*NOECHO
*CONSTITUTIVE   0
*ELEMENTS      28
         3
*NODES         40
*BOUNDARY_C    19
*HARDENING      5
*FORCE         10
*END
*ITERATION
     20       .01       10.0       .01
*ELEMENT         3
    1    1     5     6     2
    2    2     6    21    17
    3   17    21     7     3
    4    3     7     8     4
    5    5    18    22     6
    6    6    22    27    25
    7    6    25    39    21
    8   21    39    37     7
    9   37    35    24     7
   10    7    24    20     8
   11   25    27    28    26
   12   25    26    40    39
   13   39    40    38    37
   14   38    36    35    37
   15   18     9    10    22
   16   22    10    29    27
   17   29    10    23    31
   18   31    23    11    33
   19   33    11    24    35
```

```
   20   24   11   12   20
   21   27   29   30   28
   22   30   29   31   32
   23   32   31   33   34
   24   34   33   35   36
   25    9   13   14   10
   26   10   14   19   23
   27   23   19   15   11
   28   11   15   16   12
*COORDINATE
    1        0.0        0.0
    2        0.0        1.0
    3        0.0        2.0
    4        0.0        3.0
    5        1.0        0.0
    6        1.0        1.0
    7        1.0        2.0
    8        1.0        3.0
    9        2.0        0.0
   10        2.0        1.0
   11        2.0        2.0
   12        2.0        3.0
   13        3.0        0.0
   14        3.0        1.0
   15        3.0        2.0
   16        3.0        3.0
   17        0.0        1.5
   18        1.5        0.0
   19        3.0        1.5
   20        1.5        3.0
   21        1.0        1.5
   22        1.5        1.0
   23        2.0        1.5
   24        1.5        2.0
```

```
    25      1.2146      1.2146
    26      1.4293      1.4293
    27      1.5000      1.2000
    28      1.5000      1.4000
    29      1.7854      1.2146
    30      1.5707      1.4293
    31      1.8000      1.5000
    32      1.6000      1.5000
    33      1.7854      1.7854
    34      1.5707      1.5707
    35      1.5000      1.8000
    36      1.5000      1.6000
    37      1.2146      1.7854
    38      1.4293      1.5707
    39      1.2000      1.5000
    40      1.4000      1.5000
*PROPERTY
    1   40          1.0     1.0E6     0.3
*BOUNDARY_C
    1    1
    1    2
    2    1
    3    1
    4    1
   17    1
C     13    1         0.01
C     14    1         0.01
C     15    1         0.01
C     16    1         0.01
```

```
*FORCE
   13    1    10000.0
   14    1    15000.0
   19    1    10000.0
   15    1    15000.0
   16    1    10000.0
*PRINT
         TOTAL
         STRESS
         REACTION
*END
*STOP
```

Listing 3 Subelement Model

```
TEST PROBLEM FOR AN EMBEDDED HOLE ( PLANE STRESS )
*SECA
*LOUB 3 1 3
*NOECHO
*EMBED
*CONSTITUTIVE     0
*ELEMENTS         9
          3
C       101
*NODES           16
*BOUNDARY_C       9
*FORCE            4
*END
*ITERATION
     20       .1      10.0      1.00
```

```
*ELEMENT          3
    1    1     5     6    2
    2    2     6     7    3
    3    3     7     8    4
    4    5     9    10    6
    5    6    10    11    7
    6    7    11    12    8
    7    9    13    14   10
    8   10    14    15   11
    9   11    15    16   12
*COORDINATE
    1         0.0         0.0
    2         0.0         1.0
    3         0.0         2.0
    4         0.0         3.0
    5         1.0         0.0
    6         1.0         1.0
    7         1.0         2.0
    8         1.0         3.0
    9         2.0         0.0
   10         2.0         1.0
   11         2.0         2.0
   12         2.0         3.0
   13         3.0         0.0
   14         3.0         1.0
   15         3.0         2.0
   16         3.0         3.0
*PROPERTY
    1   16          1.0       1.0E6       0.3
*BOUNDARY_C
    1    1
    1    2
    2    1
    3    1
    4    1
```

```
C     13    1          0.01
C     14    1          0.01
C     15    1          0.01
C     16    1          0.01
*FORCE
   13     1     10000.0
   14     1     20000.0
   15     1     20000.0
   16     1     10000.0
*HOLE
    5     3         0.2
*PRINT
          TOTAL
          STRESS
          REACTION
*END
*STOP
```

The elastic stress field obtained by the global solution is shown in Figure 15 and qualitatively agrees with the classical solution found in many textbooks, e.g., SAVIN (1951). The elastic solution after one iteration, as summarized in Table 6, indicates that the quadratic subelement produces the most accurate results for the stress concentration factor.

ORIGINAL PAGE
COLOR PHOTOGRAPH

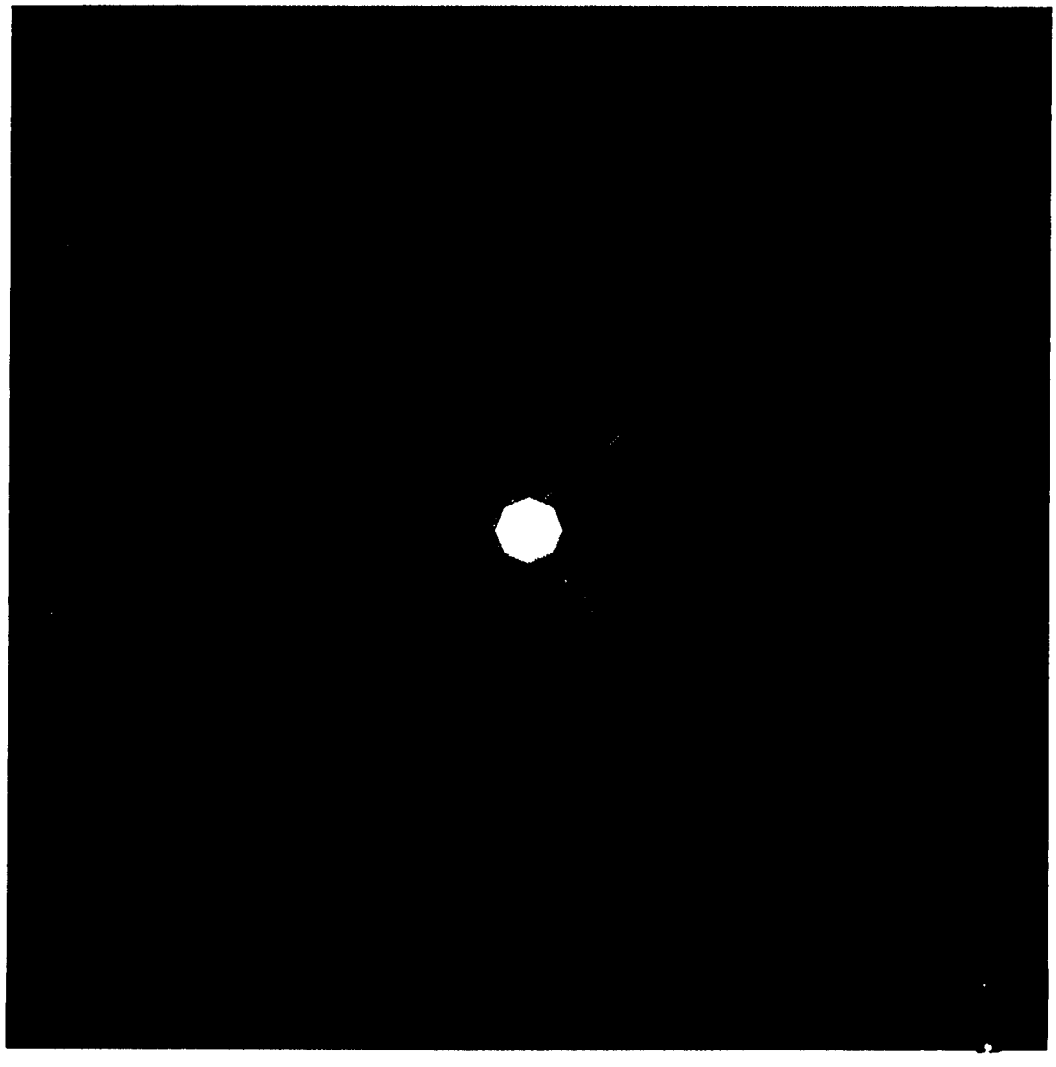

FIGURE 15 ELASTIC STRESS DISTRIBUTION FOR A PLATE WITH A HOLE

PRECEDING PAGE BLANK NOT FILMED

PAGE 70 INTENTIONALLY BLANK

Table 6 Nodal Stress Concentration Factor at the Edge of a Circular Hole After One Iteration

	Global Solution	Subelement Solution	
Point A		Linear	Quadratic
σ_x	2.2615	2.3198	2.7087
σ_y	0.5916	0.5977	0.3929
τ_{xy}	0.0002	0.0000	0.0003
Point B			
σ_x	0.1752	0.4339	-0.2702
σ_y	-0.0813	-0.2995	-0.5958
τ_{xy}	0.0000	0.0000	0.0000

For the elastic-plastic analyses, the material is assumed to be bilinear and is defined by *WORKLOAD data as:

Stress	Plastic Strain
2.0	0.0
4.0	0.4

Note that the stress here is normalized by the uniform horizontal stress for the solution of the square plate without a hole. As is well-known from standard elasticity, amplification of the horizontal stress value by a factor of 3.0 is expected at Point A under pure elastic behavior.

Both linear and quadratic subelement results, as well as global finite element results, with the same mesh, are compared. The monotonic convergence characteristics of the subelement method can be seen in these comparisons, as summarized in Table 7.

Table 7 Elastic-Plastic Analysis of a Square Plate with a Circular Hole; Nodal Stress at the Edge of the Circular Hole at Maximum SCF Location (Point A)

	Global Solution		Linear Subelement Solution		Quadratic Subelement Solution	
	Elastic	Elastic-Plastic	Elastic	Elastic-Plastic	Elastic	Elastic-Plastic
Equivalent Plastic Strain	0.0	0.0191	0.0	0.0320	0.0	0.0513
Stress						
σxx	2.3492	2.2786	2.5064	2.4151	2.7087	2.4624
σyy	0.3160	0.4339	0.4327	0.6682	0.3929	0.4929
σxy	0.0034	0.0049	0.0010	0.0009	0.0000	0.0000

Note here that iterations were carried out until a convergence tolerance of 10% in terms of relative residual was met. This solution procedure improved the elastic stress results compared to elastic results obtained earlier. The same convergence criteria were used for all calculations shown in Table 7. In comparison with solutions reported previously, the quadratic subelement method exhibited superior performance, at least for this particular example of an embedded hole.

5.0 REFERENCES

Babuska, I., O. C. Zienkiewicz, J. Gago and E. R. de A. Oliveira (eds.), Accuracy Estimates and Adaptive Refinements in Finite Element Computations, Wiley, Chichester, 1986.

Babuska, I., "The Finite Element Method with Lagrange Multipliers," Numer. Math., 20, 1973, pp. 179-192.

Bathe, K. J. and E. L. Wilson, Numerical Methods in Finite Element Analysis, Prentice Hall, Englewood Cliffs, New Jersey, 1976.

Bazeley, G. P., Y. K. Cheung, B. M. Irons and O. C. Zienkiewicz, "Triangular Elements in Plate Bending. Conforming and Non-Conforming Solutions," Proc. 1st Conf. Matrix Methods in Structural Mechanics, AFFDL-TR-CC-80, 1966, pp. 547-576.

Belytschko, T., "A Review of Recent Developments in Plate and Shell Elements," Computational Mechanics - Advances and Trends (ed. A. K. Noor), ASME AMD - Vol. 75, 1986, pp. 217-232.

Benson, D. J. and J. O. Hallquist, "A Simple Rigid Body Algorithm for Structural Dynamics Programs," Int. J. Num. Meth. Eng., 22, 1986, pp. 723-749.

Brezzi, F., "On the Existence, Uniqueness and Approximation of Saddle-Point Problems Arising from Lagrange Multipliers," RAIRO, 22, 1974, pp. 129-151.

Brown, P. N. and A. C. Hindmarsh, "Matrix-Free Methods for Stiff System of ODE's," SIAM J. Numer. Anal., 23, 1986, pp. 610-638.

Fyhre, D. and T. J. R. Hughes, "A Literature Survey on Finite Element Methodology for Turbine Engine Hot Section Components," MARC Analysis Research Corporation, Palo Alto, California, 1983.

Gaudreau, G. L., D. J. Benson, J. O. Hallquist, G. J. Kay, R. W. Rosinsky and S. J. Sachett, "Supercomputers for Engineering Analysis," Computational Mechanics - Advances and Trends (ed. A. K. Noor), ASME AMD - Vol. 75, 1986, pp. 117-131.

Hayes, L. J. and P. Devloo, "A Vectorized Version of a Spare Matrix-Vector Multiply," Int. J. Num. Meth. Eng., 23, 1986, pp. 1043-1056.

Hu, H. C., "On Some Variational Principles in the Theory of Elasticity and Plasticity," Scintia Sinica, 4, 1955, pp. 33-54.

Hughes, T. J. R. and W. K. Liu, "Nonlinear Finite Element Analysis of Shells; Part I: Three Dimensional Shells," Comp. Meth. Appl. Mech. Eng., 26, 1981, pp. 331-362.

Hughes, T. J. R., "Analysis of Transient Algorithms with Particular Reference to Stability Behavior," Computational Methods for Transient Analysis (eds. T. Belytschko and T. J. R. Hughes), Chap. 2, North-Holland, Amsterdam, 1983.

Hughes, T. J. R. and F. Shakie, "Pseudo-Corner Theory: A Simple Enhancement of J_2 - Flow Theory for Applications Involving Non-Proportional Loading," Eng. Comp., 3, 1986, pp. 116-120.

Hughes, T. J. R., R. M. Ferencz and J. O. Hallquist, "Large-Scale Vectorized Implicit Calculations in Solid Mechanics on a CRAY X-MP/48 Utilizing EBE Preconditioned Conjugate Gradients," Computational Mechanics - Advances and Trends (ed. A. K. Noor), ASME AMD - Vol. 75, 1986, pp. 233-279.

Jameson, A., "Current Status and Future Directions of Computational Transonics," Computational Mechanics - Advances and Trends (ed. A. K. Noor), ASME AMD - Vol. 75, 1986, pp. 329-368.

Kawai, T. and N. Yoshimura, "Analysis of Large Deflection of Plates by Finite Element Method," Int. J. Num. Meth. Eng., 1, 1969, pp. 123-133.

Le Tallec, P., "Mixed Numerical Methods in Viscoplasticity," Proc. 1st WCCM, Vol. 1, Texas Institute for Computational Mechanics, 1986.

Lohner, R., "FEM-FCT and Adaptive Refinement Schemes for Strongly Unsteady Flows," Numerical Methods for Compressible Flows - Finite Difference, Element and Volume Techniques (eds. T. E. Tezduyar and T. J. R. Hughes), ASME AMD - Vol. 78, 1986, pp. 93-114.

Nagtegaal, J. C. and J. G. Slater, "A Simple Non-Compatible Thin Shell Element Based on Discrete Kirchhoff Theory," Nonlinear Finite Element Analysis of Plates and Shells (ed. T. J. R. Hughes, A. Pifko and A. Jay), ASME AMD - Vol. 48, 1981, pp. 167-192.

Nagtegaal, J. C., S. Nakazawa and M. Tateishi, "On the Construction of Optimal Mindlin Type Shell Elements," Finite Element Methods for Plate and Shell Structures, Vol. 1: Element Technology (eds. T. J. R. Hughes and E. Hinton), Pineridge Press, Swansea, 1986, pp. 348-364.

Nakazawa, S., 3-D Inelastic Analysis Methods for Hot Section Components, Third Annual Status Report; Volume 1: Special Finite Element Models, NASA CR-179494, Pratt & Whitney PWA-5940-46, 1986.

Nakazawa, S. and J. C. Nagtegaal, "An Efficient Numerical Procedure for Nonlinear Analysis of Turbine Engine Hot Section Components," presented at 3rd Symp. on Nonlinear Constitutive Relations for High Temperature Applications, Akron, Ohio, 1986.

Nakazawa, S. and M. S. Spiegel, "Mixed Finite Elements and Iterative Solution Processes," presented at 1st WCCM, Austin, Texas, 1986.

Needleman, A., "Finite Element Analysis of Failure Modes in Ductile Solids," Proc. 1st WCCM, Vol. 1, Texas Institute for Computational Mechanics, 1986.

Nour-Omid, B. and M. Ortiz, "Concurrent Solution Methods for Finite Element Equations," Proc. 1st WCCM, Vol. 1, Texas Institute for Computational Mechanics, 1986.

Ortiz, M. and Y. Leroy, "A Finite Element Method for Localized Failure Analysis," Proc. 1st WCCM, Vol. 1, Texas Institute for Computational Mechanics, 1986.

Ortiz, M. and J. C. Simo, "An Analysis of a New Class of Integration Algorithms for Elastoplastic Constitutive Relations," Int. J. Num. Meth. Eng., 23, 1986, pp. 355-366.

Peraire, J., K. Morgan and O. C. Zienkiewicz, "Convection Dominated Problems," Numerical Methods for Compressible Flows - Finite Difference, Element and Volume Techniques (eds. T. E. Tezduyar and T. J. R. Hughes), ASME AMD - Vol. 78, 1986, pp. 129-147.

Pian, T. H. H. (ed.), Special Memorial Issue Dedicated to Prof. Kyuichiro Washizu, Computers and Structures, 19 (1/2), 1984.

Rawtani, S. and M. A. Dokainish, "Natural Frequencies of Rotating Low Aspect Ratio Turbomachinery Blades," AIAA Paper 71-374, Anaheim, California, 1971.

Savin, G. N., Stress Concentration Around Holes (in Russian, 1951), English Edition by Pergamon Press, London, 1961.

Simo, J. C., "Regular Perturbation Schemes for the Iterative Solution of Symmetric Eigenvalue Problems," Manuscript, Applied Mechanics Division, Stanford University, 1985.

Simo, J. C., "A Framework for Finite Strain Elastoplasticity Based on Maximum Plastic Dissipation and the Multiplicative Decomposition. Part I: Continuum Formulation; Part II: Computational Aspects," Manuscript, Applied Mechanics Division, Stanford University, 1985.

Stummel, F., "The Limitations of Patch Test," Int. J. Num. Meth. Eng., 15, 1980, pp. 177-188.

Taylor, R. L., "Solution of Linear Equations by a Profile Solver," Eng. Comp., 2, 1985, pp. 344-350.

Taylor, R. L., J. C. Simo, O. C. Zienkiewicz and A. C. H. Chen, "The Patch Test - A Condition for Assessing FEM Convergence," Int. J. Num. Meth. Eng., 22, 1986, pp. 39-62.

Thomas, J. and C. A. Mota Soares, "Finite Element Analysis of Rotating Shells," ASME Paper 73-DET-94, 1973.

Utku, S., M. Salama and R. J. Melosh, "Concurrent Cholesky Factorization of Positive Definite Banded Hermitian Matrices," Int. J. Num. Meth. Eng., 23, 1986, pp. 2137-2152.

Utku, S., R. J. Melosh, M. Salama and H. T. Chang, "Problem Decomposition for Parallel Processing," Proc. 1st WCCM, Vol. 1, Texas Institute for Computational Mechanics, 1986.

Washizu, K., On the Variational Principles of Elasticity and Plasticity, Technical Report 25-18, Aeroelastic and Struct. Res. Lab., Massachusetts Institute of Technology, 1955.

Washizu, K., Variational Methods in Elasticity and Plasticity, Pergamon Press, Oxford, 1974.

Way, S., "Uniformly Loaded, Clamped, Rectangular Plates with Large Deformation," Proc. 5th Int'l. Cong. Appl. Mech., Cambridge, Massachusetts, 1938.

William, K., N. Sobh and S. Sture, "Bifurcation Studies of Elastic-Plastic Solids," Proc. 1st WCCM, Vol. 1, Texas Institute for Computational Mechanics, 1986.

Wilson, R. B., M. J. Bak, S. Nakazawa and P. K. Banerjee, 3-D Inelastic Analysis Methods for Hot Section Components (Base Program), First Annual Status Report, NASA CR-174700, 1984.

Wilson, R. B., M. J. Bak, S. Nakazawa and P. K. Banerjee, 3-D Inelastic Analysis Methods for Hot Section Components (Base Program), Second Annual Status Report, NASA CR-175060, 1985.

Zienkiewicz, O. C., The Finite Element Method, 3rd Edition, McGraw-Hill, New York, 1977.

Zienkiewicz, O. C. and S. Nakazawa, "On Variational Formulation and Its Modifications for Numerical Solution," Computers and Structures, 19, 1984, pp. 303-313.

Zienkiewicz, O. C., X. K. Li and S. Nakazawa, "Dynamic Transient Analysis by a Mixed, Iterative Method," Int. J. Num. Meth. Eng., 23, 1986, pp. 1343-1353.

Zienkiewicz, O. C., Three-Field Mixed Approximation and the Plate Bending Problem, Report No. C/R/566/86, Institute for Numerical Method in Engineering, University College of Swansea, 1986.

Zienkiewicz, O. C., S. Qu, R. L. Taylor and S. Nakazawa, "The Patch Test for Mixed Formulations," Int. J. Num. Meth. Eng., 23, 1986, pp. 1873-1883.

Zienkiewicz, O. C. and J. Z. Zhu, "A Simple Error Estimator and Adaptive Procedure for Practical Engineering Analysis," Int. J. Num. Meth. Eng., 24, 1987, pp. 337-357.

Zyvoloski, G., "Incomplete Factorization for Finite Element Methods," Int. J. Num. Meth. Eng., 23, 1986, pp. 1101-1109.

DISTRIBUTION LIST

NASA-Lewis Research Center
Attn: Contracting Officer, MS 500-313
21000 Brookpark Road
Cleveland, OH 44135

NASA-Lewis Research Center
Attn: Tech Rpt Control Office, MS 60-1
21000 Brookpark Road
Cleveland, OH 44135

NASA-Lewis Research Center
Attn: Tech Utilization Office, MS 7-3
21000 Brookpark Road
Cleveland, OH 44135

NASA-Lewis Research Center
Attn: AFSC Liaison Office, MS 501-3
21000 Brookpark Road
Cleveland, OH 44135

NASA-Lewis Research Center
Attn: Div. Contract File, MS 49-6
21000 Brookpark Road
Cleveland, OH 44135 (2 copies)

NASA-Lewis Research Center
Attn: Library, MS 60-3
21000 Brookpark Road
Cleveland, OH 44135

NASA-Lewis Research Center
Attn: C. C. Chamis, MS 49-8
21000 Brookpark Road
Cleveland, OH 44135 (2 copies)

NASA-Lewis Research Center
Attn: L. Berke, MS 49-6
21000 Brookpark Road
Cleveland, OH 44135

NASA-Lewis Research Center
Attn: R. E. Kielb, MS 49-8
21000 Brookpark Road
Cleveland, OH 44135

NASA-Lewis Research Center
Attn: G. R. Halford, MS 49-7
21000 Brookpark Road
Cleveland, OH 44135

NASA-Lewis Research Center
Attn: D. A. Hopkins, MS 49-8
21000 Brookpark Road
Cleveland, OH 44135 (2 copies)

NASA-Lewis Research Center
Attn: R. H. Johns, MS 49-8
21000 Brookpark Road
Cleveland, OH 44135

NASA-Lewis Research Center
Attn: D. E. Sokolowski, MS 49-7
21000 Brookpark Road
Cleveland, OH 44135

NASA-Lewis Research Center
Attn: R. L. Thompson, MS 49-8
21000 Brookpark Road
Cleveland, OH 44135

NASA-Lewis Research Center
Attn: R. C. Bill, MS 77-12
21000 Brookpark Road
Cleveland, OH 44135

NASA Headquarters
Attn: NHS-22/Library
600 Independence Avenue, S.W.
Washington, DC 20546

NASA Headquarters
Attn: R/S. L. Venneri
600 Independence Avenue, S.W.
Washington, DC 20546

NASA Headquarters
Attn: R/M. S. Hirschbein
600 Independence Avenue, S.W.
Washington, DC 20546

NASA S&T Information Facility
Attn: Acquisition Dept. (10 copies)
P. O. Box 8757
Balt.-Wash. Int. Airport, MD 21240

NASA Ames Research Center
Attn: Library, MS 202-3
Moffett Field, CA 94035

DISTRIBUTION LIST (continued)

NASA Goddard Space Flight Center
Attn: 252/Library
Greenbelt, MD 20771

NASA John F. Kennedy Space Center
Attn: Library, AD-CSO-1
Kennedy Space Center, FL 32931

NASA Langley Research Center
Attn: Library, MS 185
Hampton, VA 23665

NASA Langley Research Center
Attn: J. Starnes
Hampton, VA 23665

NASA Lyndon B. Johnson Space Center
Attn: JM6/Library
Houston, TX 77001

NASA George C. Marshall Space
Flight Center
Attn: L. Kiefling
Marshall Space Flt. Center, AL 35812

Jet Propulsion Laboratory
Attn: B. Wada
4800 Oak Grove Drive
Pasadena, CA #91103

Air Force Aeronautical Propulsion
Laboratory
Attn: Z. Gershon
Wright-Patterson AFB, OH 45433

Air Force Systems Command
Attn: C. W. Cowie
Aeronautical Systems Division
Wright-Patterson AFB, OH 45433

Air Force Systems Command
Attn: R. J. Hill
Aeronautical Systems Division
Wright-Patterson AFB, OH 45433

U.S. Army Ballistics Research Lab.
Attn: Dr. D. F. Haskell, DRXBR-BM
Aberdeen Proving Ground, MD 21005

Mechanics Research Laboratory
Attn: Dr. E. M. Lenoe
Army Mat'ls & Mech. Research Center
Watertown, MA 02172

National Bureau of Standards
Attn: R. Mitchell
Engineering Mechanics Section
Washington, DC 20234

U.S. Army Missile Command
Attn: Document Section
Redstone Scientific Info Center
Redstone Arsenal, AL 35808

Commanding Officer
U.S. Army Research Office (Durham)
Box CM, Duke Station (Attn: Library)
Durham, NC 27706

Department of the Army
Attn: AMCRD-RC
U.S. Army Material Command
Washington, DC 20315

Bureau of Naval Weapons
Department of the Navy
Attn: RRRE-6
Washington, DC 20360

Commander, U.S. Naval Ordnance Lab.
Attn: Library
White Oak
Silver Springs, MD 20910

Director, Code 6180
U.S. Naval Research Laboratory
Attn: Library
Washington, DC 20390

Naval Air Propulsion Test Center
Aeronautical Engine Department
Attn: Mr. James Salvino
Trenton, NJ 08628

DISTRIBUTION LIST (continued)

Denver Federal Center
U.S. Bureau of Reclamation
Attn: P. M. Lorenz
P. O. Box 25007
Denver, CO 80225

FAA, ARD-520
Attn: Commander John J. Shea
2100 Second Street, SW
Washington, DC 20591

Federal Aviation Administration DOT
Office of Aviation Safety, FOB 1 OA
Attn: Mr. John H. Enders
800 Independence Avenue, SW
Washington, DC 20594

Federal Aviation Administration
Code ANE-214, Propulsion Section
Attn: Mr. Robert Berman
12 New England Executive Park
Burlington, MA 01803

National Transportation Safety Board
Attn: Edward P. Wizniak, MS TE-20
800 Independence Avenue, SW
Washington, DC 20594

Aeronautical Research Association
of Princeton, Inc.
Attn: Dr. Thomas McDonough
P. O. Box 2229
Princeton, NJ 08540

Aerospace Corporation
Attn: Library-Documents
2400 E. El Segundo Blvd.
Los Angeles, CA 90045

Allison Gas Turbine Operation
General Motors Corporation
Attn: Mr. William Springer
Speed Code T3, Box 894
Indianapolis, IN 46206

Allison Gas Turbine Operation
General Motors Corporation
Attn: Mr. L. Snyder
Speed Code T3, Box 894
Indianapolis, IN 46206

AVCO Lycoming Division
Attn: Mr. Herbert Kaehler
550 South Main Street
Stratford, CT 06497

Boeing Aerospace Company
Impact Mechanics Lab
Attn: Dr. R. J. Bristow
P. O. Box 3999
Seattle, WA 98124

Boeing Commercial Airplane Company
Attn: Dr. Ralph B. McCormick
P. O. Box 3707
Seattle, WA 98124

Bell Aerospace
Attn: R. A. Gellatly
P. O. Box 1
Buffalo, NY 14240

Bell Aerospace
Attn: S. Gellin
P. O. Box 1
Buffalo, NY 14240

Beech Aircraft Corporation,
Plant 1
Attn: Mr. M. K. O'Connor
Wichita, KA 67201

Boeing Commercial Airplane Company
Attn: David T. Powell, MS 73-01
P. O. Box 3707
Seattle, WA 98124

Boeing Commercial Airplane Company
Attn: Dr. John H. Gerstle
P. O. Box 3707
Seattle, WA 98124

Boeing Company
Attn: Mr. C. F. Tiffany
Wichita, KA 67201

Douglas Aircraft Company
Attn: M. A. O'Connor, Jr., MS 36-41
3855 Lakewood Blvd.
Long Beach, CA 90846

Garrett AiResearch Manufacturing Co.
Attn: L. A. Matsch
111 S. 34th Street
P. O. Box 5217
Phoenix, AZ 85010

General Dynamics
Attn: Library
P. O. Box 748
Fort Worth, TX 76101

General Dynamics/Convair Aerospace
Attn: Library
P. O. Box 1128
San Diego, CA 92112

General Electric Company
Attn: Dr. L. Beitch, MS K221
Interstate 75, Bldg. 500
Cincinnati, OH 45215

General Electric Company
Attn: Dr. R. L. McKnight, MS K221
Interstate 75, Bldg. 500
Cincinnati, OH 45215

General Electric Company
Attn: Dr. M. Roberts, MS K221
Interstate 75, Bldg. 500
Cincinnati, OH 45215

General Electric Company
Aircraft Engine Group
Attn: Mr. Herbert Garten
Lynn, MA 01902

General Motors Corporation
Attn: R. J. Tippet
Warren, MI 48090

Grumman Aircraft Engineering
Corporation
Attn: Library
Bethpage, Long Island, NY 11714

Grumman Aircraft Engineering
Corporation
Attn: H. A. Armen
Bethpage, Long Island, NY 11714

Lawrence Livermore Laboratory
Attn: Library
P. O. Box 808, L-421
Livermore, CA 94550

Lawrence Livermore Laboratory
Attn: M. L. Wilkins
P. O. Box 808, L-421
Livermore, CA 94550

Arthur D. Little
Acorn Park
Attn: P. D. Hilton
Cambridge, MA 02140

Lockheed California Company
Attn: Mr. D. T. Pland
P. O. Box 551
Dept. 73-31, Bldg. 90, Plant A-1
Burbank, CA 91520

Lockheed California Company
Attn: Mr. Jack E. Wignot
P. O. Box 551
Dept. 73-31, Bldg. 90, Plant A-1
Burbank, CA 91520

DISTRIBUTION LIST (continued)

Lockheed Palo Alto Research
Laboratories
Attn: D. Bushnell
Palo Alto, CA 94304

Lockheed Palo Alto Research
Laboratories
Attn: R. F. Hurtung
Palo Alto, CA 94304

Lockheed Missiles and Space Company
Huntsville Research & Eng. Center
Attn: W. Armstrong
P. O. Box 1103
Huntsville, AL 35807

MacNeal-Schwendler Corporation
Attn: R. H. MacNeal
7442 North Figueroa Street
Los Angeles, CA 90041

MARC Analysis Research Corporation
Attn: P. V. Marcel
260 Sheridan Avenue, Suite 314
Palo Alto, CA 94306

Northrop Space Laboratories
Attn: Library
3401 West Broadway
Hawthorne, CA 90250

North American Rockwell, Inc.
Space & Information Systems Div.
Attn: Library
12214 Lakewood Blvd.
Downey, CA 90241

Norton Company
Attn: Mr. George E. Buron
Industrial Ceramics Div.
Armore & Spectramic Products
Worcester, MA 01606

Norton Company
Attn: Mr. Paul B. Gardner
1 New Bond Street
Industrial Ceramics Div.
Worcester, MA 01606

Republic Aviation
Fairchild Hiller Corporation
Attn: Library
Farmington, Long Island, NY

Rohr Industries
Attn: Mr. John Meaney
Foot of H Street
Chula Vista, CA 92010

Southwest Research Institute
Attn: Dr. T. A. Cruse
P. O. Box 28510
Culebra Road
San Antonio, TX 78284

Solar Turbine Inc.
Attn: G. L. Padgett
P. O. Box 80966
San Diego, CA 92138

Cleveland State University
Attn: Dr. P. Bellino
Department of Civil Engineering
Cleveland, OH 44115

Rockwell International Corporation
Attn: J. Gausselin, D422/402AB71
Los Angeles International Airport
Los Angeles, CA 90009

Rockwell International Corporation
Rocketdyne Division
Attn: J. F. Newell
6633 Canoga Avenue
Canoga Park, CA 91304

Rockwell International Corporation
Rocketdyne Division
Attn: K. R. Rajagopal
6633 Canoga Avenue
Canoga Park, CA 91304

TWA, Inc.
Attn: Mr. John J. Morelli
Kansas City International Airport
P. O. Box 20126
Kansas City, MO 64195

Pratt & Whitney
Attn: Library, MS 732-11
P. O. Box B269
West Palm Beach, FL 33402

Pratt & Whitney
Attn: R. A. Marmol, MS 713-39
P. O. Box B269
West Palm Beach, FL 33402

Pratt & Whitney
Attn: Library, MS 169-31
400 Main Street
East Hartford, CT 06108

Pratt & Whitney
Attn: E. S. Todd, MS 163-09
400 Main Street
East Hartford, CT 06108

United Technologies Corporation
Hamilton Standard
Attn: Dr. R. A. Cornell
Windsor Locks, CT 06096

United Technologies Research Center
Attn: Dr. A. Dennis, MS 18
Silver Lane
East Hartford, CT 06108

Westinghouse R&D Center
Attn: N. E. Dowling
1310 Beulah Road
Pittsburgh, PA 15235

Westinghouse Adv. Energy Sys. Div.
Attn: P. T. Falk
Waltz Mill
P. O. Box 158
Madison, PA 15663

University of Akron
Department of Civil Engineering
Attn: Dr. Paul Chang
Akron, OH 44325

University of Arizona
College of Engineering
Attn: H. Kamel
Tucson, AZ 87521

University of California
Department of Civil Engineering
Attn: E. Wilson
Berkeley, CA 94720

University of Dayton
Research Institute
Attn: F. K. Bogner
Dayton, OH 45409

Georgia Institute of Technology
School of Civil Engineering
Attn: S. N. Atluri
Atlanta, GA 30332

Georgia Institute of Technology
Attn: G. J. Simitsis
225 North Avenue
Atlanta, GA 30332

Georgia Institute of Technology
Attn: R. L. Calson
225 North Avenue
Atlanta, GA 30332

Lehigh University Institute of
Fracture and Solid Mechanics
Attn: G. T. McAllister
Bethlehem, PA 18015

Univ. of Illinois at Chicago Circle
Dept. of Materials Engineering
Attn: Dr. Robert L. Spilker
Box 4348
Chicago, IL 60680

University of Kansas
School of Engineering
Attn: R. H. Dodds
Lawrence, KS 66045

DISTRIBUTION LIST (continued)

Massachusetts Institute of Technology
Attn: J. Mar
Cambridge, MA 02139

State University of New York at Buffalo
Department of Civil Engineering
Attn: P. K. Banerjee
Buffalo, NY 14225

State University of New York at Buffalo
Department of Civil Engineering
Attn: R. Shaw
Buffalo, NY 14214

Purdue University
School of Aeronautics & Astronautics
Attn: C. T. Sun
West Lafayette, IN 47907

V. P. I. and State University
Department of Engineering Mechanics
Attn: R. H. Heller
Blacksburg, VA 24061

Rensselaer Polytechnic Institute
Attn: R. Loewy
Troy, NY 12181

Stanford University
School of Engineering
Attn: T. J. R. Hughes
Stanford, CA 94305

Texas A&M University
Aerospace Engineering Department
Attn: W. E. Haisler
College Station, TX 77843

University of Texas at Austin
College of Engineering
Attn: J. T. Oden
Austin, TX 78712-1085